

## Symmetry modes and description of distorted phases in hexagonal $ABX_3$ compounds. Application to $\text{KNiCl}_3$ room-temperature structure

J. L. Mañes, M. J. Tello, and J. M. Pérez-Mato

*Departamento de Física, Facultad de Ciencias, Universidad del País Vasco, Apdo 644, Bilbao, Spain*

(Received 26 January 1982)

The group-theoretical analysis of the hexagonal perovskite structure ( $3L$ , space group  $P6_3/mmc$ ), considered as a common prototype phase of most hexagonal or pseudo-hexagonal  $ABX_3$  compounds, which was initiated recently [Pérez-Mato *et al.*, J. Phys. C **14**, 1121 (1981)], is continued in this paper. After discussing, in a general case, the distortion created by a structural phase transition in terms of symmetry modes of the prototype structure, the selection rules restricting their presence in the distortion are formulated stressing the role played by the invariance groups of the prototype-space-group irreducible representations. Then, restricting the study to the hexagonal perovskite structure, we have worked out its symmetry modes and their compatibility relations. Finally, as an example, the room-temperature phase in  $\text{KNiCl}_3$  is analyzed as a distortion from the ideal hexagonal perovskite. The possible nine symmetry modes intervening in it are described, and their relative weight in the actual distortion is calculated. Although the crystal is separated by about 260 K from the nearest reported phase transition, the distortion is surprisingly dominated by the two modes corresponding to the necessary order-parameter symmetry describing the symmetry change between the compared phases, while the amplitudes of the remaining "free" modes are at least 1 order of magnitude smaller.

### I. INTRODUCTION

It is well known that many compounds with the general formula  $ABX_3$  undergo structural phase transitions corresponding to slight distortions of the ideal cubic or hexagonal perovskites ( $3L$  or  $2L$ ) structures with  $Pm\ 3m$  or  $P6_3/mmc$  symmetries, respectively. In the case of the cubic-prototype phase there are some phase-transition sequences that have been widely and intensively investigated in the past. See, for example, a short review about  $ABCl_3$  compounds in Ref. 1. In more recent years interesting phase transitions have also been found in  $ABX_3$  compounds with a hexagonal or pseudo-hexagonal-prototype phase.<sup>2-5</sup> It is likely that in the future new phase transitions will be discovered. This expectation and the already important number of known phase transitions in this group make a wide theoretical study based on symmetry arguments desirable.

According to this idea, we recently presented<sup>6</sup> a systematic study of the possible phase symmetries derived from a prototype phase with the  $P6_3/mmc$  space group. In that paper all the irreducible representations (IR) of the prototype space group that

belong to symmetry points in the hexagonal Brillouin zone were analyzed as possible order-parameter (OP) symmetries, and all their invariance groups<sup>7</sup> were obtained.

In this paper, the symmetry arguments are extended to the description of the structural characteristics of the low-symmetry phases in the hexagonal  $ABX_3$  compounds. The microscopic variables (modes) that describe the low-symmetry phase as a structural distortion of the prototype phase are investigated. The theory is discussed in a general form in Sec. II, where the important role that symmetry modes play in the formalism is shown. Subsequently the symmetry modes and their compatibility relationships have been determined for the hexagonal perovskite  $ABX_3$  structure, and the results are summarized in several tables in Sec. III and Appendixes A, B, and C. All symmetry points and lines in the hexagonal Brillouin zone have been treated. Finally, in Sec. IV, the recently reported room-temperature structure of  $\text{KNiCl}_3$  is analyzed as an example, making use of the results presented in preceding sections and Ref. 6. Throughout the paper, the employed notation follows closely that of Bradley and Cracknell<sup>8</sup> and Maradudin and Vosko.<sup>9</sup>

## II. CRYSTAL STRUCTURE DISTORTION ANALYSIS

Among the set of microscopic variables in a crystal, the symmetry modes of the prototype phase are in most cases fundamental for the description of the phase-transition mechanisms. They are relevant not only in the case of displacive transitions, where the softening of a vibrational mode plays an important role, but also in a general case, since they can always be used to describe the idealized structural distortion that relates the low-temperature phase with the prototype phase. In this section we shortly develop the mathematical structure of this description, following similar lines and notation of those employed in Ref. 9 for the analysis of crystal vibrational normal modes. In this way we introduce the equations and notation that are to be used in Sec. III to determine and express the symmetry modes for the hexagonal  $ABX_3$  structure.

A distortion in a crystal structure with  $N$  unit

cells and  $r$  atoms in each can be described by the displacements from their ideal sites of its  $Nr$  atoms:

$$u_\alpha(lk), \quad (1)$$

where  $\alpha = x, y, z, l = 1, \dots, N, k = 1, \dots, r$ . These quantities can be considered as vector components of a  $3Nr$ -dimensional linear space  $M$ , in which a representation  $\mathcal{M}$  of the crystal (without distortions) space group  $G$  can be readily defined.

In order to obtain a total reduction of  $\mathcal{M}$  and the bases for the IR, let us consider "Bloch-wave" distortions of the form

$$u_\alpha(lk) = U_\alpha(k | \vec{K}_1) \exp[i\vec{K}_1 \cdot \vec{x}(l)]. \quad (2)$$

The transformation properties of  $U_\alpha(k | \vec{K}_1)$  can be expressed in a matrix form. If  $g = \{R | \vec{v}(R) + \vec{x}(m)\}$  is an element of  $G$ , we have

$$U_\alpha(k | R\vec{K}_1) = \Gamma_{\alpha\beta}(kk' | \vec{K}_1; g) U_\beta(k' | \vec{K}_1), \quad (3)$$

with

$$\Gamma_{\alpha\beta}(kk' | \vec{K}_1; g) = R_{\alpha\beta} \delta(k, F_0(k'; g)) \exp\{i\vec{K}_1 \cdot [g^{-1}\vec{x}(k) - \vec{x}(k')]\}, \quad (4)$$

where  $R_{\alpha\beta}$  is the matrix associated with  $R$  in the vector representation and  $F_0(k'; g)$  denotes the atoms index to which the  $k'$  atom transforms by the action of  $g$ .

According to (3), the  $3r$ -dimensional subspace  $M_{\vec{K}_1}$  ( $\vec{K}_1$  fixed) defined in (2) is invariant for those elements  $g \in G$  such that  $R\vec{K}_1 \equiv \vec{K}_1$  (little group  $G_{\vec{K}_1}$ ), and the matrices (4) describe a representation  $\mathcal{M}_{\vec{K}_1}$  of  $G_{\vec{K}_1}$  in it. This representation can be decomposed in a sum of small irreducible representations<sup>8</sup>  $D_s(\vec{K}_1, n)$  of  $G$ :

$$\mathcal{M}_{\vec{K}_1} = \sum_n m(n) D_s(\vec{K}_1, n). \quad (5)$$

We can represent the corresponding bases in the form

$$\{\vec{E}(\vec{K}_1 n t a)\}, \quad t = 1, \dots, d(n) \quad (6)$$

where  $d(n)$  is the dimension of  $D_s(\vec{K}_1, n)$  and the index  $a$  distinguishes between bases corresponding to different subspaces that transform according to the same small IR  $D_s(\vec{K}_1, n)$  when  $m(n) > 1$ . These symmetry modes transform according to their definition as follows:

$$\begin{aligned} \Gamma_{\alpha\beta}(kk' | \vec{K}_s; g) E_\beta(k' | \vec{K}_1 n t a) \\ = D_{\alpha'}(\vec{K}_1, n | g) E_\alpha(k | \vec{K}_1 n t a), \end{aligned} \quad (7)$$

where  $D_{\alpha'}(\vec{K}_1, n)$  are the matrix elements of the small IR. They can be determined by the usual projection operator techniques or from Eq. (7) as an alternative method. In fact, it is the latter that has been used in Sec. III. The basis can be readily extended to the whole  $G$ -invariant linear space

$$M_{[\vec{K}_1]} = M_{\vec{K}_1} \oplus M_{\vec{K}_2} \oplus \dots \oplus M_{\vec{K}_\sigma}$$

(where  $\vec{K}_1, \dots, \vec{K}_\sigma$  are the vectors of the  $[\vec{K}_1]$  star):

$$\{\vec{E}(\vec{K}_p n t a)\}, \quad t = 1, \dots, d(n), \quad p = 1, \dots, \sigma. \quad (8)$$

These vectors are determined by the property

$$\vec{E}(\vec{K}_p n t a) = \Gamma(\vec{K}_1; g_p) \vec{E}(\vec{K}_1 n t a), \quad (9)$$

where  $g_p$  is an arbitrary but fixed element of  $G$  such that  $R_p \vec{K}_1 = \vec{K}_p$ . For  $n$  and  $a$  fixed, the vectors (8) constitute a basis transforming according to the IR  $D(\vec{K}_1, n)$  of  $G$ , and as a whole, with  $\vec{K}_1$

variable, they define a basis in the space  $M$ . Therefore, any distortion can be written

$$u_\alpha(lk) = \sum_{(\vec{K}_1, n)} \sum_{(p, t)} \sum_a C(\vec{K}_1, npta) \times E_\alpha(k | \vec{K}_p nta) e^{i \vec{K}_p \cdot \vec{r}(l)} \quad (10)$$

In the case of Landau-type phase transitions,<sup>10</sup> the space group  $F$  of the distorted phase<sup>11</sup> is a subgroup of  $G$  formed by the set of symmetry elements which keep the OP displacement invariant. This displacement is defined in a vector space transforming according to an IR  $D_0$  of  $G$ . Obviously the distortion  $u_\alpha(lk)$  should be compatible with the new symmetry  $F$ . This means that in (10) only terms corresponding to IR  $D(\vec{K}, n)$  of  $G$ , such that they subduce the identity representation in  $F$ , will be present. That is, their subduction index<sup>6</sup>  $S(F | \vec{K}, n)$  should be not null.<sup>12</sup> We shall call these IR compatible representations (with  $F$ ).

In fact, this restriction in (10) is equivalent to saying, in a manner closer to Von Neumann's principle, that the symmetry modes triggered by the transition are those belonging to an IR of  $G$  that have invariance groups containing  $F$  as a subgroup (this includes obviously the proper IR  $D_0$  of the OP). Also, the relationship between the symmetry coordinates  $C(\vec{K}_1, npta)$  should be such that the "displacement" in the IR space takes place along the subspace corresponding to the invariance group containing  $F$ .

Therefore, in our particular case, where  $P6_3/mmc$  is the prototype group, the determination of the compatible IR relevant in (10) and the relationships between the coefficients for a given phase transition is reduced to a search in the tables from Ref. 6, where the invariance groups of all the symmetry-point IR were listed, as well as the corresponding subspaces.

With respect to the temperature dependence of the symmetry coordinate  $C(\vec{K}_1, npta)$ , they can be considered as "faint variables" (Refs. 13–16) for which the thermodynamic part of the standard Landau theory predicts near the phase transition (if continuous) a behavior proportional to  $(T - T_0)^f$ , where  $T_0$  is the transition temperature and  $f$  the so-called faintness index of the corresponding IR.<sup>7,15</sup> The latter is given by the first symmetrized power of  $[D_0]^f$  in which the considered IR appears.

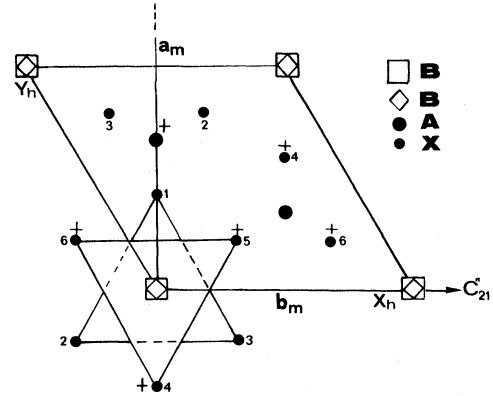


FIG. 1. Schematic representation of the hexagonal perovskite structure  $ABX_3$  ( $2L$ ).

### III. SYMMETRY MODES IN THE HEXAGONAL PEROVSKITE STRUCTURE

The hexagonal perovskite structure, which can be considered the prototype phase for most of the hexagonal  $ABX_3$  compounds, is represented in Fig. 1. The atoms in the unit cell are labeled by letters and numbers. The symmetry modes for this type of structure, as well as their compatibility relations for symmetry points and lines of the hexagonal Brillouin zone, are shown in this section and Appendixes A, B, and C. Although these calculations, according to what is stated in Sec. II, have been performed keeping in mind their application to the description of phase transitions in the hexagonal  $ABX_3$  structures, it should be noted that the information presented here can be used in any other physical situation where the symmetry modes of this structure are needed. Furthermore, the conclusions from this section can be extended to any other crystal with  $P6_3/mmc$  symmetry for those atoms with the same site symmetries as the atoms of our particular case, which are shown in Table I.

Owing to the properties of the vector representation and the distinguishability of the atoms, the  $M$  space defined in Sec. II can be divided in our case

TABLE I. Site symmetries in Wyckoff notation for the hexagonal perovskite ( $2L$ ).

Atom	Site	Point-group symmetry
A	a	$3m$
B	d	$\bar{6}m2$
X	h	$mm$

TABLE II. Symmetry modes corresponding to the  $A$  and  $B$  ions along the  $z$  axis. The vector components are given in the order  $(A_{1z}, A_{2z})$  and  $(B_{1z}, B_{2z})$ , respectively.

$\Gamma$	$\underline{A}_{2u}$	$(1,1)/\sqrt{2}$	$u_1$	$\Gamma$	$\underline{A}_{2u}$	$(1,1)/\sqrt{2}$	$u_{31}$
	$\underline{B}_{1u}$	$(1,-1)/\sqrt{2}$	$u_2$		$\underline{B}_{2g}$	$(1,-1)/\sqrt{2}$	$u_{32}$
$M$	$\underline{M}_3^-$	$(1,1)/\sqrt{2}$	$u_3$	$M$	$\underline{M}_3^+$	$(1,1)/\sqrt{2}$	$u_{33}$
	$\underline{M}_4^-$	$(1,-1)/\sqrt{2}$	$u_4$		$\underline{M}_3^-$	$(1,-1)/\sqrt{2}$	$u_{34}$
$A$	$\underline{A}_1$	$(1,-i)/\sqrt{2}$	$u_5$	$A$	$\underline{A}_1$	$(1,-i)/\sqrt{2}$	$u_{35}$
		$(-1,-i)/\sqrt{2}$	$u_6$			$(-i,1)/\sqrt{2}$	$u_{36}$
$L$	$\underline{L}_1$	$(0,1)$	$u_7$	$L$	$\underline{L}_1$	$(1,-1)/\sqrt{2}$	$u_{37}$
		$(1,0)$	$u_8$			$(1,1)/\sqrt{2}$	$u_{38}$
$K$	$\underline{K}_2$	$(1,-1)/\sqrt{2}$	$u_9$	$K$	$\underline{K}_6$	$(1,-\omega^*)/\sqrt{2}$	$u_{39}$
	$\underline{K}_4$	$(1,1)/\sqrt{2}$	$u_{10}$			$(i, i\omega^*)/\sqrt{2}$	$u_{40}$
$H$	$\underline{H}_3$	$(1,-1)/\sqrt{2}$	$u_{11}$	$H$	$\underline{H}_2$	$(0,1)$	$u_{41}$
		$(-i,-i)/\sqrt{2}$	$u_{12}$			$(i\omega, 0)$	$u_{42}$
$\Delta$	$\underline{A}_1$	$(1,\lambda)/\sqrt{2}$	$u_{13}$	$\Delta$	$\underline{A}_1$	$(1,\lambda)/\sqrt{2}$	$u_{43}$
$(e^{i\pi\alpha})$	$\underline{B}_1$	$(1,-\lambda)/\sqrt{2}$	$u_{14}$	$(e^{i\pi\alpha})$	$\underline{B}_1$	$(1,-\lambda)/\sqrt{2}$	$u_{44}$
$U$	$\underline{U}_1$	$(1,\lambda)/\sqrt{2}$	$u_{15}$	$U$	$\underline{U}_1$	$(1,-\lambda)/\sqrt{2}$	$u_{45}$
$(e^{i\pi\alpha})$	$\underline{U}_2$	$(1,-\lambda)/\sqrt{2}$	$u_{16}$	$(e^{i\pi\alpha})$	$\underline{U}_2$	$(1,\lambda)/\sqrt{2}$	$u_{46}$
$P$	$\underline{P}_1$	$(1,\lambda)/\sqrt{2}$	$u_{17}$	$P$	$\underline{P}_3$	$(1,\omega^*\lambda)/\sqrt{2}$	$u_{47}$
$(e^{i\pi\alpha})$	$\underline{P}_2$	$(1,-\lambda)/\sqrt{2}$	$u_{18}$	$(e^{i\pi\alpha})$		$(-i, i\omega^*\lambda)/\sqrt{2}$	$u_{48}$
$T$	$\underline{T}_2$	$(1,1)/\sqrt{2}$	$u_{19}$	$T$	$\underline{T}_2$	$(1,\lambda)/\sqrt{2}$	$u_{49}$
	$\underline{T}_4$	$(1,-1)/\sqrt{2}$	$u_{20}$	$(e^{i2\pi\alpha})$	$\underline{T}_3$	$(1,-\lambda)/\sqrt{2}$	$u_{50}$
$S$	$\underline{S}_1$	$(0,1)$	$u_{21}$	$S$	$\underline{S}_1$	$(1,\lambda)/\sqrt{2}$	$u_{51}$
		$(i,0)$	$u_{22}$	$(e^{i2\pi\alpha})$		$(i,-i\lambda)/\sqrt{2}$	$u_{52}$
$T'$	$\underline{T}_2'$	$(1,1)/\sqrt{2}$	$u_{23}$	$T'$	$\underline{T}_2'$	$(1,-\lambda)/\sqrt{2}$	$u_{53}$
	$\underline{T}_4'$	$(1,-1)/\sqrt{2}$	$u_{24}$	$(e^{i2\pi\alpha})$	$\underline{T}_3'$	$(1,\lambda)/\sqrt{2}$	$u_{54}$
$S'$	$\underline{S}_1'$	$(0,1)$	$u_{25}$	$S'$	$\underline{S}_1'$	$(1,-\lambda)/\sqrt{2}$	$u_{55}$
		$(i,0)$	$u_{26}$	$(e^{i2\pi\alpha})$		$(i, i\lambda)/\sqrt{2}$	$u_{56}$
$\Sigma$	$\underline{\Sigma}_1$	$(1,-1)/\sqrt{2}$	$u_{27}$	$\Sigma$	$\underline{\Sigma}_2$	$(1,0)$	$u_{57}$
					$\underline{\Sigma}_2$	$(0,1)$	$u_{58}$
	$\underline{\Sigma}_2$	$(1,1)/\sqrt{2}$	$u_{28}$				
$R$	$^1\underline{E}'$	$(1,-1)/\sqrt{2}$	$u_{29}$	$R$	$^1\underline{E}'$	$(0,1)$	$u_{59}$
	$^2\underline{E}'$	$(1,1)/\sqrt{2}$	$u_{30}$		$^2\underline{E}'$	$(1,0)$	$u_{60}$

into the following invariant subspaces:

$$M = A_z \oplus A_{xy} \oplus B_z \oplus B_{xy} \oplus X_z \oplus X_{xy} . \quad (11)$$

Therefore each subspace can be treated separately. The symmetry modes have been obtained from a

systematic application of Eq. (7) and are listed in detail in Tables II–VI.<sup>17</sup> The matrices used for the small IR at the symmetry points were constructed from the tables in Ref. 8 and coincide with those used in our previous paper.<sup>6</sup> The com-

TABLE III. Symmetry modes for the  $A$  ions in the  $xy$  plane. The vector components are given in the order ( $A_{1x}, A_{1y}, A_{2x}, A_{2y}$ ), except for symmetry lines  $T$  and  $S$ , where the components are given along the  $x'$  and  $y'$  axes (see Fig. 2).

$\Gamma$	$\underline{E}_{1u}$	$(1,0,1,0)/\sqrt{2}$	$u_{61}$	$P$ $(e^{i\pi\alpha})$	$\underline{P}_3$	$(0,1,0,\lambda)/\sqrt{2}$	$u_{93}$
		$(0,1,0,1)/\sqrt{2}$	$u_{62}$			$(-1,0,-\lambda,0)/\sqrt{2}$	$u_{94}$
	$\underline{E}_{2u}$	$(0,1,0,-1)/\sqrt{2}$	$u_{63}$		$\underline{P}_3$	$(1,0,-\lambda,0)/\sqrt{2}$	$u_{95}$
		$(1,0,-1,0)/\sqrt{2}$	$u_{64}$			$(0,1,0,-\lambda)/\sqrt{2}$	$u_{96}$
$M$	$\underline{M}_1^-$	$(0,1,0,-1)/\sqrt{2}$	$u_{65}$	$T$	$\underline{T}_1$	$(0,1,0,1)/\sqrt{2}$	$u_{97}$
	$\underline{M}_2^-$	$(0,1,0,1)/\sqrt{2}$	$u_{66}$		$\underline{T}_2$	$(1,0,-1,0)/\sqrt{2}$	$u_{98}$
	$\underline{M}_3^-$	$(1,0,-1,0)/\sqrt{2}$	$u_{67}$		$\underline{T}_3$	$(0,1,0,-1)/\sqrt{2}$	$u_{99}$
	$\underline{M}_4^-$	$(1,0,1,0)/\sqrt{2}$	$u_{68}$		$\underline{T}_4$	$(1,0,1,0)/\sqrt{2}$	$u_{100}$
$A$	$\underline{A}_3$	$(1,i,-i,1)/2$	$u_{69}$	$S$	$\underline{S}_1$	$(0,0,1,0)$	$u_{101}$
		$(-1,i,-i,-1)/2$	$u_{70}$			$(-i,0,0,0)$	$u_{102}$
		$(1,-i,-i,-1)/2$	$u_{71}$		$\underline{S}_1$	$(0,1,0,0)$	$u_{103}$
		$(-1,-i,-i,1)/2$	$u_{72}$			$(0,0,0,-i)$	$u_{104}$
$L$	$\underline{L}_1$	$(0,0,1,0)$	$u_{73}$	$T'$	$\underline{T}'_1$	$(0,1,0,1)/\sqrt{2}$	$u_{105}$
		$(-1,0,0,0)$	$u_{74}$			$(1,0,-1,0)/\sqrt{2}$	$u_{106}$
	$\underline{L}_2$	$(0,0,0,1)$	$u_{75}$		$\underline{T}'_2$	$(0,1,0,-1)/\sqrt{2}$	$u_{107}$
		$(0,-1,0,0)$	$u_{76}$		$\underline{T}'_4$	$(1,0,1,0)/\sqrt{2}$	$u_{108}$
$K$	$\underline{K}_5$	$(0,1,0,1)/\sqrt{2}$	$u_{77}$	$S'$	$\underline{S}'_1$	$(0,0,1,0)$	$u_{109}$
		$(-1,0,-1,0)/\sqrt{2}$	$u_{78}$			$(-i,0,0,0)$	$u_{110}$
	$\underline{K}_6$	$(0,1,0,-1)/\sqrt{2}$	$u_{79}$		$\underline{S}'_1$	$(0,1,0,0)$	$u_{111}$
		$(1,0,-1,0)/\sqrt{2}$	$u_{80}$			$(0,0,0,-i)$	$u_{112}$
$H$	$\underline{H}_1$	$(1,i,1,i)/2$	$u_{81}$	$\Sigma$	$\underline{\Sigma}_1$	$(1,0,1,0)/\sqrt{2}$	$u_{113}$
		$(i,1,-i,-1)/2$	$u_{82}$			$(1,0,-1,0)/\sqrt{2}$	$u_{114}$
	$\underline{H}_2$	$(1,-i,1,-i)/2$	$u_{83}$		$\underline{\Sigma}_2$	$(0,1,0,-1)/\sqrt{2}$	$u_{115}$
		$(-i,1,i,-1)/2$	$u_{84}$			$(0,1,0,1)/\sqrt{2}$	$u_{116}$
$\Delta$ $(e^{i\pi\alpha})$	$\underline{E}_1$	$(1,0,\lambda,0)/\sqrt{2}$	$u_{85}$	$R$	$\underline{\Sigma}_3$	$(1,0,1,0)/\sqrt{2}$	$u_{117}$
		$(0,1,0,\lambda)/\sqrt{2}$	$u_{86}$			$(1,0,-1,0)/\sqrt{2}$	$u_{118}$
	$\underline{E}_2$	$(1,0,-\lambda,0)/\sqrt{2}$	$u_{87}$		$\underline{\Sigma}_4$	$(0,1,0,-1)/\sqrt{2}$	$u_{119}$
		$(0,-1,0,\lambda)/\sqrt{2}$	$u_{88}$			$(0,1,0,1)/\sqrt{2}$	$u_{120}$
$U$ $(e^{i\pi\alpha})$	$\underline{U}_1$	$(1,0,-\lambda,0)/\sqrt{2}$	$u_{89}$	$R$	$^1E'$	$(1,0,1,0)/\sqrt{2}$	$u_{117}$
	$\underline{U}_2$	$(1,0,\lambda,0)/\sqrt{2}$	$u_{90}$		$^2E'$	$(1,0,-1,0)/\sqrt{2}$	$u_{118}$
	$\underline{U}_3$	$(0,1,0,-\lambda)/\sqrt{2}$	$u_{91}$		$^1E''$	$(0,1,0,-1)/\sqrt{2}$	$u_{119}$
	$\underline{U}_4$	$(0,1,0,\lambda)/\sqrt{2}$	$u_{92}$		$^2E''$	$(0,1,0,1)/\sqrt{2}$	$u_{120}$

patibility relations gathered in Appendix B were used as an auxiliary method and a consistence check for the calculated symmetry modes. Some of the relations in Appendix B were previously given by Kroese<sup>18</sup> in a different notation and have been included here for the sake of completeness. The symmetry vectors in Tables II–VI are described by the atomic displacements in the origin unit cell ( $l=0$ ). The displacements are given along the  $(x,y,z)$  axes except for  $T$  and  $S$  lines where the

set  $(x',y',z')$  is used (see Fig. 2). Each table corresponds to a subspace in (11) and the particular details are explained in the table.

The vectors have been numbered to facilitate any later reference. Some modes corresponding to symmetry lines are stated as a function of  $\lambda$ , which is given by the exponential under the letter denoting the symmetry line. In this exponential,  $\alpha$  refers to a particular  $\vec{K}_1$  vector along the line. It must also be noted that when a representation ap-

TABLE IV. Symmetry modes of the  $B$  ions in the  $xy$  plane. Notations:  $(B_{1x}, B_{1y}, B_{2x}, B_{2y})$ , except for symmetry lines  $T$  and  $S$ , where the components are given along the  $x'$  and  $y'$  axes (see Fig. 2).

$\Gamma$	$\underline{E}_{1u}$	$(1,0,1,0)/\sqrt{2}$	$u_{121}$	$(e^{i\pi\alpha})$	$\underline{U}_3$	$(0,1,0,\lambda)/\sqrt{2}$	$u_{151}$
		$(0,1,0,1)/\sqrt{2}$	$u_{122}$		$\underline{U}_4$	$(0,1,0,-\lambda)/\sqrt{2}$	$u_{152}$
	$\underline{E}_{2g}$	$(1,0,-1,0)/\sqrt{2}$	$u_{123}$				
		$(0,-1,0,1)/\sqrt{2}$	$u_{124}$	$P$	$\underline{P}_1$	$(1,-i,-\omega^*\lambda,-i\omega^*\lambda)/2$	$u_{153}$
$M$	$\underline{M}_1^+$	$(1,0,1,0)/\sqrt{2}$	$u_{125}$	$(e^{i\pi\alpha})$	$\underline{P}_2$	$(1,-i,\omega^*\lambda,i\omega^*\lambda)/2$	$u_{154}$
	$\underline{M}_3^+$	$(0,1,0,1)/\sqrt{2}$	$u_{126}$		$\underline{P}_3$	$(1,i,-\omega^*\lambda,i\omega^*\lambda)/2$	$u_{155}$
	$\underline{M}_2^-$	$(0,1,0,-1)/\sqrt{2}$	$u_{127}$			$(i,-1,i\omega^*\lambda,\omega^*\lambda)/2$	$u_{156}$
	$\underline{M}_4^-$	$(1,0,-1,0)/\sqrt{2}$	$u_{128}$	$T$	$\underline{T}_1$	$(1,0,-\lambda,0)/\sqrt{2}$	$u_{157}$
$A$	$\underline{A}_3$	$(1,i,-i,1)/2$	$u_{129}$	$(e^{i2\pi\alpha})$	$\underline{T}_1$	$(0,1,0,\lambda)/\sqrt{2}$	$u_{158}$
		$(-i,-1,1,-i)/2$	$u_{130}$		$\underline{T}_4$	$(1,0,\lambda,0)/\sqrt{2}$	$u_{159}$
		$(1,-i,-i,-1)/2$	$u_{131}$		$\underline{T}_4$	$(0,1,0,-\lambda)/\sqrt{2}$	$u_{160}$
		$(-i,1,1,i)/2$	$u_{132}$	$S$	$\underline{S}_1$	$(1,0,\lambda,0)/\sqrt{2}$	$u_{161}$
$L$	$\underline{L}_1$	$(1,0,-1,0)/\sqrt{2}$	$u_{133}$	$(e^{i2\pi\alpha})$	$\underline{S}_1$	$(-i,0,i\lambda,0)/\sqrt{2}$	$u_{162}$
		$(-1,0,-1,0)/\sqrt{2}$	$u_{134}$			$(0,-1,0,\lambda)/\sqrt{2}$	$u_{163}$
	$\underline{L}_2$	$(0,1,0,-1)/\sqrt{2}$	$u_{135}$			$(0,i,0,i\lambda)/\sqrt{2}$	$u_{164}$
		$(0,-1,0,-1)/\sqrt{2}$	$u_{136}$	$T'$	$\underline{T}'_1$	$(1,0,\lambda,0)/\sqrt{2}$	$u_{165}$
$K$	$\underline{K}_1$	$(1,-i,-\omega^*, -i\omega^*)/2$	$u_{137}$	$(e^{i2\pi\alpha})$	$\underline{T}'_1$	$(0,1,0,-\lambda)/\sqrt{2}$	$u_{166}$
	$\underline{K}_2$	$(1,-i,\omega^*, i\omega^*)/2$	$u_{138}$		$\underline{T}'_4$	$(1,0,-\lambda,0)/\sqrt{2}$	$u_{167}$
	$\underline{K}_5$	$(1,i,-\omega^*, i\omega^*)/2$	$u_{139}$		$\underline{T}'_4$	$(0,1,0,\lambda)/\sqrt{2}$	$u_{168}$
		$(i,-1,i\omega^*, \omega^*)/2$	$u_{140}$	$S'$	$\underline{S}'_1$	$(1,0,-\lambda,0)/\sqrt{2}$	$u_{169}$
$H$	$\underline{H}_2$	$(1,i,0,0)/\sqrt{2}$	$u_{141}$	$(e^{i2\pi\alpha})$	$\underline{S}'_1$	$(-i,0,-i\lambda,0)/\sqrt{2}$	$u_{170}$
		$(0,0,i\omega^*, \omega^*)/\sqrt{2}$	$u_{142}$			$(0,-1,0,-\lambda)/\sqrt{2}$	$u_{171}$
	$\underline{H}_3$	$(1,-i,0,0)/\sqrt{2}$	$u_{143}$			$(0,i,0,-i\lambda)/\sqrt{2}$	$u_{172}$
		$(0,0,i\omega^*, -\omega^*)/\sqrt{2}$	$u_{144}$	$\Sigma$	$\underline{\Sigma}_1$	$(1,0,0,0)$	$u_{173}$
$\Delta$	$\underline{E}_1$	$(1,0,\lambda,0)/\sqrt{2}$	$u_{145}$		$\underline{\Sigma}_1$	$(0,0,1,0)$	$u_{174}$
		$(0,1,0,\lambda)/\sqrt{2}$	$u_{146}$		$\underline{\Sigma}_4$	$(0,1,0,0)$	$u_{175}$
	$(e^{i\pi\alpha}) \underline{E}_2$	$(1,0,-\lambda,0)/\sqrt{2}$	$u_{147}$		$\underline{\Sigma}_4$	$(0,0,0,1)$	$u_{176}$
		$(0,-1,0,\lambda)/\sqrt{2}$	$u_{148}$	$R$	$^1\underline{E}'$	$(1,0,0,0)$	$u_{177}$
$U$	$\underline{U}_1$	$(1,0,\lambda,0)/\sqrt{2}$	$u_{149}$		$^2\underline{E}'$	$(0,0,1,0)$	$u_{178}$
	$\underline{U}_2$	$(1,0,-\lambda,0)/\sqrt{2}$	$u_{150}$		$^1\underline{E}''$	$(0,0,0,1)$	$u_{179}$
					$^2\underline{E}''$	$(0,1,0,0)$	$u_{180}$

pears several times in a subspace, the symmetry modes have been taken as orthogonal in order to simplify their use. Furthermore, in those points ( $L$  and  $M$ ) and lines ( $R$ ,  $U$ ,  $\Sigma$ ,  $S'$ ,  $T'$ ,  $S$ , and  $T$ ) where the displacement subspace in the  $xy$  plane can be separated into invariant subspaces along the  $x$  and  $y$  axes ( $x'$  and  $y'$  for  $S$  and  $T$ ), each decomposition appears separately in the table, and the corresponding modes are constructed according to this separation. For example, in the  $M$  point we have for the  $X_{xy}$  subspace (see Appendix B, Table XVII):

$$X_x = 2M_1^+ + 2M_4^- + M_3^+ + M_2^- ,$$

and

$$X_y = M_1^+ + M_4^+ + 2M_3^- + 2M_2^- .$$

Therefore we can consider a  $M_3^+(x)$  mode ( $U_{287}$  in Table VI) and two  $M_3^+(y)$  modes ( $U_{286}$  and  $U_{288}$ , also in Table VI).

All modes can be directly taken from Tables II–VI, except for those corresponding to the  $\Delta$ ,  $U$ , and  $K$  symmetry lines in the  $X_{xy}$  subspace. In

TABLE V. Symmetry modes for the  $X$  ions along the  $z$  axis. Notation:  $(X_{1z}, X_{2z}, X_{3z}, X_{4z}, X_{5z}, X_{6z})$ . As in preceding tables, for symmetry lines  $T$  and  $S$ , the vector components are given along the  $x'$  and  $y'$  axes. The form of the vectors in  $T$  and  $T'$ ,  $S$  and  $S'$  coincide.

$\Gamma$	$\underline{A}_{2u}$	$(1, 1, 1, 1, 1, 1)/\sqrt{6}$	$u_{181}$
	$\underline{B}_{2g}$	$(1, 1, 1, -1, -1, -1)/\sqrt{6}$	$u_{182}$
	$\underline{E}_{1g}$	$(0, \sqrt{3}, -\sqrt{3}, 0, -\sqrt{3}, \sqrt{3})/2\sqrt{3}$	$u_{183}$
		$(-2, 1, 1, 2, -1, -1)/2\sqrt{3}$	$u_{184}$
	$\underline{E}_{2u}$	$(0, \sqrt{3}, -\sqrt{3}, 0, \sqrt{3}, -\sqrt{3})/2\sqrt{3}$	$u_{185}$
		$(2, -1, -1, 2, -1, -1)/2\sqrt{3}$	$u_{186}$
$M$	$\underline{M}_2^+$	$(1, 0, 0, -1, 0, 0)/\sqrt{2}$	$u_{187}$
	$\underline{M}_2^+$	$(0, 1, 1, 0, -1, -1)/2$	$u_{188}$
	$\underline{M}_2^+$	$(0, 1, -1, 0, -1, 1)/2$	$u_{189}$
	$\underline{M}_1^-$	$(0, 1, -1, 0, 1, -1)/2$	$u_{190}$
	$\underline{M}_3^-$	$(1, 0, 0, 1, 0, 0)/\sqrt{2}$	$u_{191}$
	$\underline{M}_3^-$	$(0, 1, 1, 0, 1, 1)/2$	$u_{192}$
$A$	$\underline{A}_1$	$(1, 1, 1, -i, -i, -i)/\sqrt{6}$	$u_{193}$
		$(-i, -i, -i, 1, 1, 1)/\sqrt{6}$	$u_{194}$
	$\underline{A}_3$	$(1, \omega, \omega^*, i, i\omega, i\omega^*)/\sqrt{6}$	$u_{195}$
		$(i, i\omega^*, i\omega, 1, \omega^*, \omega)/\sqrt{6}$	$u_{196}$
		$(1, \omega^*, \omega, i, i\omega^*, i\omega)/\sqrt{6}$	$u_{197}$
		$(i, i\omega, i\omega^*, 1, \omega, \omega^*)/\sqrt{6}$	$u_{198}$
$L$	$\underline{L}_1$	$(1, 0, 0, 1, 0, 0)/\sqrt{2}$	$u_{199}$
		$(1, 0, 0, -1, 0, 0)/\sqrt{2}$	$u_{200}$
	$\underline{L}_1$	$(0, 1, 1, 0, 1, 1)/2$	$u_{201}$
		$(0, 1, 1, 0, -1, -1)/2$	$u_{202}$
	$\underline{L}_2$	$(0, 1, -1, 0, 1, -1)/2$	$u_{203}$
		$(0, 1, -1, 0, -1, 1)/2$	$u_{204}$
$K$	$\underline{K}_3$	$(1, 1, 1, -1, -1, -1)/\sqrt{6}$	$u_{205}$
	$\underline{K}_4$	$(1, 1, 1, 1, 1, 1)/\sqrt{6}$	$u_{206}$
	$\underline{K}_6$	$(1, \omega, \omega^*, -1, -\omega^*, -\omega)/\sqrt{6}$	$u_{207}$
		$(i, i\omega, i\omega^*, i, i\omega^*, i\omega)/\sqrt{6}$	$u_{208}$
	$\underline{K}_6$	$(1, \omega^*, \omega, -1, -\omega, -\omega^*)/\sqrt{6}$	$u_{209}$
		$(-i, -i\omega^*, -i\omega, -i, -i\omega, -i\omega^*)/\sqrt{6}$	$u_{210}$
$H$	$\underline{H}_1$	$(0, 0, 0, 1, \omega, \omega^*)/\sqrt{3}$	$u_{211}$
		$(-i, -i\omega^*, -i\omega, 0, 0, 0)/\sqrt{3}$	$u_{212}$
	$\underline{H}_2$	$(0, 0, 0, 1, \omega^*, \omega)/\sqrt{3}$	$u_{213}$
		$(i, i\omega, i\omega^*, 0, 0, 0)/\sqrt{3}$	$u_{214}$
	$\underline{H}_3$	$(0, 0, 0, 1, 1, 1)/\sqrt{3}$	$u_{215}$
		$(i, i, i, 0, 0, 0)/\sqrt{3}$	$u_{216}$
$\Delta$ ( $e^{i\pi\alpha}$ )	$\underline{A}_1$	$(1, 1, 1, \lambda, \lambda, \lambda)/\sqrt{6}$	$u_{217}$
	$\underline{B}_1$	$(1, 1, 1, -\lambda, -\lambda, -\lambda)/\sqrt{6}$	$u_{218}$
	$\underline{E}_1$	$(2, -1, -1, -2\lambda, \lambda, \lambda)/2\sqrt{3}$	$u_{219}$
		$(0, \sqrt{3}, -\sqrt{3}, 0, -\sqrt{3}\lambda, \sqrt{3}\lambda)/2\sqrt{3}$	$u_{220}$

these cases the modes are obtained from the compatibility relations and the modes for the  $\Gamma$ ,  $M$ , and  $K$  points. For instance, the  $U_3(x)$  mode, according to Table XVII in Appendix B, is compatible with  $M_3^+(x)$ , and  $M_3^+(x)$  from Table VI is

given by

$$U_{287} = (0, 0, 1, 0, -1, 0, 0, 0, -1, 0, 1, 0)/2.$$

As it is stated in the table, the factor  $\lambda = e^{i\pi\alpha}$  must

TABLE V. (Continued.)

	$E_2$	$(2, -1, -1, 2\lambda, -\lambda, -\lambda)/2\sqrt{3}$ $(0, -\sqrt{3}, \sqrt{3}, 0, -\sqrt{3}\lambda, \sqrt{3}\lambda)/2\sqrt{3}$	$u_{221}$ $u_{222}$
$U$  $(e^{i\pi\alpha})$	$U_1$	$(1, 0, 0, \lambda, 0, 0)/\sqrt{2}$	$u_{223}$
	$U_1$	$(0, 1, 1, 0, \lambda, \lambda)/2$	$u_{224}$
	$U_2$	$(1, 0, 0, -\lambda, 0, 0)/\sqrt{2}$	$u_{225}$
	$U_2$	$(0, 1, 1, 0, -\lambda, -\lambda)/2$	$u_{226}$
	$U_3$	$(0, 1, -1, 0, \lambda, -\lambda)/2$	$u_{227}$
	$U_4$	$(0, 1, -1, 0, -\lambda, \lambda)/2$	$u_{228}$
$P$  $(e^{i\pi\alpha})$	$P_1$	$(1, 1, 1, 1, 1, 1)/\sqrt{6}$	$u_{229}$
	$P_2$	$(1, 1, 1, -1, -1, -1)/\sqrt{6}$	$u_{230}$
	$P_3$	$(1, \omega, \omega^*, \lambda, \omega^* \lambda, \omega \lambda)/\sqrt{6}$	$u_{231}$
		$(-i, -i\omega, -i\omega^*, i\lambda, i\omega^* \lambda, i\omega \lambda)/\sqrt{6}$	$u_{232}$
	$P_3$	$(1, \omega^*, \omega, \lambda, \omega \lambda, \omega^* \lambda)/\sqrt{6}$	$u_{233}$
		$(i, i\omega^*, i\omega, -i\lambda, -i\omega \lambda, -i\omega^* \lambda)/\sqrt{6}$	$u_{234}$
$T(T')$	$T_2(T'_2)$	$(1, 0, 0, 1, 0, 0)/\sqrt{2}$	$u_{235}(247)$
	$T_2(T'_2)$	$(0, 1, 0, 0, 1, 0)/\sqrt{2}$	$u_{236}(248)$
	$T_2(T'_2)$	$(0, 0, 1, 0, 0, 1)/\sqrt{2}$	$u_{237}(249)$
	$T_3(T'_3)$	$(1, 0, 0, -1, 0, 0)/\sqrt{2}$	$u_{238}(250)$
	$T_3(T'_3)$	$(0, 1, 0, 0, -1, 0)/\sqrt{2}$	$u_{239}(251)$
	$T_3(T'_3)$	$(0, 0, 1, 0, 0, -1)/\sqrt{2}$	$u_{240}(252)$
$S(S')$	$S_1(S'_1)$	$(1, 0, 0, 1, 0, 0)/\sqrt{2}$	$u_{241}(258)$
		$(1, 0, 0, -i, 0, 0)/\sqrt{2}$	$u_{242}(254)$
	$S_1(S'_1)$	$(0, 1, 0, 0, 0, 1)/\sqrt{2}$	$u_{243}(255)$
		$(0, i, 0, 0, 0, -i)/\sqrt{2}$	$u_{244}(256)$
	$S_1(S'_1)$	$(0, 0, 1, 0, 1, 0)/\sqrt{2}$	$u_{245}(257)$
		$(0, 0, i, 0, -i, 0)/\sqrt{2}$	$u_{246}(258)$
$\Sigma$	$\Sigma_2$	$(1, 0, 0, 0, 0, 0)$	$u_{259}$
	$\Sigma_2$	$(0, 0, 0, 1, 0, 0)$	$u_{260}$
	$\Sigma_2$	$(0, 1, 1, 0, 0, 0)/\sqrt{2}$	$u_{261}$
	$\Sigma_2$	$(0, 0, 0, 1, 1, 0)/\sqrt{2}$	$u_{262}$
	$\Sigma_3$	$(0, 1, -1, 0, 0, 0)/\sqrt{2}$	$u_{263}$
	$\Sigma_3$	$(0, 0, 0, 0, 1, -1)/\sqrt{2}$	$u_{264}$
$R$	$^1E'$	$(0, 0, 0, 1, 0, 0)$	$u_{265}$
	$^2E'$	$(1, 0, 0, 0, 0, 0)$	$u_{266}$
	$^1E'$	$(0, 0, 0, 0, 1, 1)/\sqrt{2}$	$u_{267}$
	$^2E'$	$(0, 1, 1, 0, 0, 0)/\sqrt{2}$	$u_{268}$
	$^1E''$	$(0, 1, -1, 0, 0, 0)/\sqrt{2}$	$u_{269}$
	$^2E''$	$(0, 0, 0, 0, 1, -1)/\sqrt{2}$	$u_{270}$

multiply the displacements of atoms 4, 5, and 6.  
Therefore, the  $U_3(x)$  mode is

$$U_{358} = (0, 0, 1, 0, -1, 0, 0, 0, -\lambda, 0, \lambda, 0)/2,$$

where the subindex is given by (287–283)

+355=358, as it follows from the labels given to the  $M$  modes (283–294) and those reserved for the  $U$  modes (355–366) (see Table VI).

Finally, it must be noted that the displacements in the tables refer to the  $l=0$  unit cell. For other

TABLE VI. Symmetry modes for the  $X$  ions in the  $xy$  plane. Notation:  $(X_{1x}, X_{1y}, X_{2x}, X_{2y}, \dots, X_{6y})$ . Modes in  $\Delta$ ,  $U$ , and  $P$  have the same form as those corresponding to  $\Gamma$ ,  $M$ , and  $K$ , respectively, except for the factor  $\lambda = e^{i\pi\alpha}$ , which should multiply the vector components of ions, 4, 5, and 6. The notation reserved for these modes is as follows.  $\Delta$ :  $u_{343} - u_{354}$ .  $U$ :  $u_{355} - u_{366}$ .  $P$ :  $u_{367} - u_{378}$ . In lines  $T$  and  $S$  the  $x'$  and  $y'$  axes are used again.

$\Gamma$	$\underline{A}_{1g}$	$(2, 0, -1, \sqrt{3}, -1, -\sqrt{3}, -2, 0, 1, -\sqrt{3}, 1, \sqrt{3})/2\sqrt{6}$	$u_{271}$
	$\underline{A}_{2g}$	$(0, 2, -\sqrt{3}, -1, \sqrt{3}, -1, 0, -2, \sqrt{3}, 1, -\sqrt{3}, 1)/2\sqrt{6}$	$u_{272}$
	$\underline{B}_{1u}$	$(2, 0, -1, \sqrt{3}, -1, -\sqrt{3}, 2, 0, -1, \sqrt{3}, -1, -\sqrt{3})/2\sqrt{6}$	$u_{273}$
	$\underline{B}_{2u}$	$(0, 2, -\sqrt{3}, -1, \sqrt{3}, -1, 0, 2, -\sqrt{3}, -1, \sqrt{3}, -1)/2\sqrt{6}$	$u_{274}$
	$\underline{E}_{1u}$	$(1, 0, 1, 0, 1, 0, 1, 0, 1, 0, 1, 0)/\sqrt{6}$	$u_{275}$
		$(0, 1, 0, 1, 0, 1, 0, 1, 0, 1, 0, 1)/\sqrt{6}$	$u_{276}$
	$\underline{E}_{1u}$	$(2, 0, -1, -\sqrt{3}, -1, \sqrt{3}, 2, 0, -1, -\sqrt{3}, -1, \sqrt{3})/2\sqrt{6}$	$u_{277}$
		$(0, -2, -\sqrt{3}, 1, \sqrt{3}, 1, 0, -2, -\sqrt{3}, 1, \sqrt{3}, 1)/2\sqrt{6}$	$u_{278}$
	$\underline{E}_{2g}$	$(1, 0, 1, 0, 1, 0, -1, 0, -1, 0, -1, 0)/\sqrt{6}$	$u_{279}$
		$(0, -1, 0, -1, 0, -1, 0, 1, 0, 1, 0, 1)/\sqrt{6}$	$u_{280}$
	$\underline{E}_{2g}$	$(2, 0, -1, -\sqrt{3}, -1, \sqrt{3}, -2, 0, 1, \sqrt{3}, 1, -\sqrt{3})/2\sqrt{6}$	$u_{281}$
		$(0, 2, \sqrt{3}, -1, -\sqrt{3}, -1, 0, -2, -\sqrt{3}, 1, \sqrt{3}, 1)/2\sqrt{6}$	$u_{282}$
$M$	$\underline{M}_1^+$	$(1, 0, 0, 0, 0, 0, -1, 0, 0, 0, 0, 0)/\sqrt{2}$	$u_{283}$
	$\underline{M}_1^+$	$(0, 0, 1, 0, 1, 0, 0, 0, -1, 0, -1, 0)/2$	$u_{284}$
	$\underline{M}_1^+$	$(0, 0, 0, 1, 0, -1, 0, 0, 0, -1, 0, 1)/2$	$u_{285}$
	$\underline{M}_3^+$	$(0, 1, 0, 0, 0, 0, 0, -1, 0, 0, 0, 0)/\sqrt{2}$	$u_{286}$
	$\underline{M}_3^+$	$(0, 0, 1, 0, -1, 0, 0, 0, -1, 0, 1, 0)/2$	$u_{287}$
	$\underline{M}_3^+$	$(0, 0, 0, 1, 0, 1, 0, 0, 0, -1, 0, -1)/2$	$u_{288}$
	$\underline{M}_2^-$	$(0, 1, 0, 0, 0, 0, 0, 1, 0, 0, 0, 0)/\sqrt{2}$	$u_{289}$
	$\underline{M}_2^-$	$(0, 0, 1, 0, -1, 0, 0, 0, 1, 0, -1, 0)/2$	$u_{290}$
	$\underline{M}_2^-$	$(0, 0, 0, 1, 0, 1, 0, 0, 0, 1, 0, 1)/2$	$u_{291}$
	$\underline{M}_4^-$	$(1, 0, 0, 0, 0, 0, 1, 0, 0, 0, 0, 0)/\sqrt{2}$	$u_{292}$
	$\underline{M}_4^-$	$(0, 0, 1, 0, 1, 0, 0, 0, 1, 0, 1, 0)/2$	$u_{293}$
	$\underline{M}_4^-$	$(0, 0, 0, 1, 0, -1, 0, 0, 0, 1, 0, -1)/2$	$u_{294}$
$A$	$\underline{A}_1$	$(2, 0, -1, \sqrt{3}, -1, -\sqrt{3}, 2i, 0, -i, \sqrt{3}i, -i, -\sqrt{3}i)/2\sqrt{6}$	$u_{295}$
		$(2i, 0, -i, \sqrt{3}i, -i, -\sqrt{3}i, 2, 0, -1, \sqrt{3}, -1, -\sqrt{3})/2\sqrt{6}$	$u_{296}$
	$\underline{A}_2$	$(0, 2, -\sqrt{3}, -1, \sqrt{3}, -1, 0, 2i, -\sqrt{3}i, -i, \sqrt{3}i, -i)/2\sqrt{6}$	$u_{297}$
		$(0, -2i, \sqrt{3}i, i, -\sqrt{3}i, i, 0, -2, \sqrt{3}, 1, -\sqrt{3}, 1)/2\sqrt{6}$	$u_{298}$
	$\underline{A}_3$	$(1, i, 1, i, 1, i, -i, 1, -i, 1, -i, 1)/2\sqrt{3}$	$u_{299}$
		$(-i, -1, -i, -1, -i, -1, 1, -i, 1, -i, 1, -i)/2\sqrt{3}$	$u_{300}$
		$(1, -i, 1, -i, 1, -i, -i, -1, -i, -1, -i, -1)/2\sqrt{3}$	$u_{301}$
		$(-i, 1, -i, 1, -i, 1, 1, i, 1, i, i, i)/2\sqrt{3}$	$u_{302}$
	$\underline{A}_3$	$(1, -i, \omega^*, -i\omega^*, \omega, -i\omega, -i, -1, -i\omega^*, -\omega^*, -i\omega, -\omega)/2\sqrt{3}$	$u_{303}$
		$(-i, 1, -i\omega, \omega, -i\omega^*, \omega^*, 1, i, \omega, i\omega, \omega^*, i\omega^*)/2\sqrt{3}$	$u_{304}$
		$(1, i, \omega, i\omega, \omega^*, i\omega^*, -i, 1, -i\omega, \omega, -i\omega^*, \omega^*)/2\sqrt{3}$	$u_{305}$
		$(-i, -1, -i\omega^*, -\omega^*, -i\omega, -\omega, 1, -i, \omega^*, -i\omega^*, \omega, -i\omega)/2\sqrt{3}$	$u_{306}$
$L$	$\underline{L}_1$	$(1, 0, 0, 0, 0, 0, 1, 0, 0, 0, 0, 0)/\sqrt{2}$	$u_{307}$
		$(-1, 0, 0, 0, 0, 0, 1, 0, 0, 0, 0, 0)/\sqrt{2}$	$u_{308}$
	$\underline{L}_1$	$(0, 0, 1, 0, 1, 0, 0, 0, 1, 0, 1, 0)/2$	$u_{309}$
		$(0, 0, -1, 0, -1, 0, 0, 0, 1, 0, 1, 0)/2$	$u_{310}$
	$\underline{L}_1$	$(0, 0, 0, 1, 0, -1, 0, 0, 0, 1, 0, -1)/2$	$u_{311}$
		$(0, 0, 0, -1, 0, 1, 0, 0, 0, 1, 0, -1)/2$	$u_{312}$
	$\underline{L}_2$	$(0, 1, 0, 0, 0, 0, 0, 1, 0, 0, 0, 0)/\sqrt{2}$	$u_{313}$
		$(0, -1, 0, 0, 0, 0, 0, 1, 0, 0, 0, 0)/\sqrt{2}$	$u_{314}$
	$\underline{L}_2$	$(0, 0, 0, 1, 0, 1, 0, 0, 0, 1, 0, 1)/2$	$u_{315}$
		$(0, 0, 0, -1, 0, -1, 0, 0, 0, 1, 0, 1)/2$	$u_{316}$
	$\underline{L}_2$	$(0, 0, 1, 0, -1, 0, 0, 0, 1, 0, -1, 0)/2$	$u_{317}$
		$(0, 0, -1, 0, 1, 0, 0, 0, 1, 0, -1, 0)/2$	$u_{318}$

TABLE VI. (Continued.)

$K$	$\underline{K}_1$	$(2, 0, -1, \sqrt{3}, -1, -\sqrt{3}, -2, 0, 1, -\sqrt{3}, 1, \sqrt{3})/2\sqrt{6}$	$u_{319}$
	$\underline{K}_1$	$(0, 2, -\sqrt{3}, -1, \sqrt{3}, -1, 0, 2, -\sqrt{3}, -1, \sqrt{3}, -1)/2\sqrt{6}$	$u_{320}$
	$\underline{K}_2$	$(2, 0, -1, \sqrt{3}, -1, -\sqrt{3}, 2, 0, -1, \sqrt{3}, -1, -\sqrt{3})/2\sqrt{6}$	$u_{321}$
	$\underline{K}_2$	$(0, 2, -\sqrt{3}, -1, \sqrt{3}, -1, 0, -2, \sqrt{3}, 1, -\sqrt{3}, 1)/2\sqrt{6}$	$u_{322}$
	$\underline{K}_5$	$(4, 0, 1, -\sqrt{3}, 1, \sqrt{3}, -4, 0, -1, \sqrt{3}, -1, -\sqrt{3})/2\sqrt{6}$	$u_{323}$
		$(0, 0, -\sqrt{3}, 3, \sqrt{3}, 3, 0, 0, \sqrt{3}, -3, -\sqrt{3}, -3)/2\sqrt{6}$	$u_{324}$
	$\underline{K}_5$	$(0, 0, \sqrt{3}, -3, -\sqrt{3}, -3, 0, 0, \sqrt{3}, -3, -\sqrt{3}, -3)/2\sqrt{6}$	$u_{325}$
		$(4, 0, 1, -\sqrt{3}, 1, \sqrt{3}, 4, 0, 1, -\sqrt{3}, 1, \sqrt{3})/2\sqrt{6}$	$u_{326}$
	$\underline{K}_5$	$(0, 4, \sqrt{3}, 1, -\sqrt{3}, 1, 0, 4, \sqrt{3}, 1, -\sqrt{3}, 1)/2\sqrt{6}$	$u_{327}$
		$(0, 0, -3, -\sqrt{3}, -3, \sqrt{3}, 0, 0, -3, -\sqrt{3}, -3, \sqrt{3})/2\sqrt{6}$	$u_{328}$
	$\underline{K}_5$	$(0, 0, 3, \sqrt{3}, 3, -\sqrt{3}, 0, 0, -3, -\sqrt{3}, -3, \sqrt{3})/2\sqrt{6}$	$u_{329}$
		$(0, 4, \sqrt{3}, 1, -\sqrt{3}, 1, 0, -4, -\sqrt{3}, -1, \sqrt{3}, -1)/2\sqrt{6}$	$u_{330}$
$H$	$\underline{H}_1$	$(2, 0, -\omega, \omega\sqrt{3}, -\omega^*, -\omega^*\sqrt{3}, 0, 0, 0, 0, 0, 0)/2\sqrt{3}$	$u_{331}$
		$(0, 0, 0, 0, 0, 0, -2i, 0, i\omega^*, -i\omega^*\sqrt{3}, i\omega, i\omega\sqrt{3})/2\sqrt{3}$	$u_{332}$
	$\underline{H}_1$	$(0, 2, -\omega\sqrt{3}, -\omega, \omega^*\sqrt{3}, -\omega^*, 0, 0, 0, 0, 0, 0)/2\sqrt{3}$	$u_{333}$
		$(0, 0, 0, 0, 0, 0, 2i, -i\omega^*\sqrt{3}, -i\omega^*, i\omega\sqrt{3}, -i\omega)/2\sqrt{3}$	$u_{334}$
	$\underline{H}^2$	$(2, 0, -\omega^*\sqrt{3}, -\omega, -\omega\sqrt{3}, 0, 0, 0, 0, 0, 0)/2\sqrt{3}$	$u_{335}$
		$(0, 0, 0, 0, 0, 0, 2i, 0, -i\omega, i\omega\sqrt{3}, -i\omega^*, -i\omega^*\sqrt{3})/2\sqrt{3}$	$u_{336}$
	$\underline{H}_2$	$(0, 2, -\omega^*\sqrt{3}, -\omega^*, \omega\sqrt{3}, -\omega, 0, 0, 0, 0, 0, 0)/2\sqrt{3}$	$u_{337}$
		$(0, 0, 0, 0, 0, 0, -2i, i\omega\sqrt{3}, i\omega, -i\omega^*\sqrt{3}, i\omega^*)/2\sqrt{3}$	$u_{338}$
	$\underline{H}_3$	$(2, 0, -1, \sqrt{3}, -1, -\sqrt{3}, 0, 0, 0, 0, 0, 0)/2\sqrt{3}$	$u_{339}$
		$(0, 0, 0, 0, 0, 0, 2i, 0, -i, \sqrt{3}i, -i, -\sqrt{3}i)/2\sqrt{3}$	$u_{340}$
$T$	$\underline{T}_1$	$(0, 2, -\sqrt{3}, -1, \sqrt{3}, -1, 0, 0, 0, 0, 0, 0)/2\sqrt{3}$	$u_{341}$
	$\underline{T}_1$	$(0, 0, 0, 0, 0, 0, -2i, \sqrt{3}i, i, -\sqrt{3}i, i)/2\sqrt{3}$	$u_{342}$
	$\underline{T}_1$	$(1, 0, 0, 0, 0, 0, 0, 0, 0, -1, 0)/\sqrt{2}$	$u_{379}$
	$\underline{T}_1$	$(0, 0, 1, 0, 0, 0, 0, 0, -1, 0, 0)/\sqrt{2}$	$u_{380}$
	$\underline{T}_1$	$(0, 0, 0, 0, 1, 0, -1, 0, 0, 0, 0)/\sqrt{2}$	$u_{381}$
	$\underline{T}_1$	$(0, 1, 0, 0, 0, 0, 0, 0, 0, 0, 1)/\sqrt{2}$	$u_{382}$
	$\underline{T}_1$	$(0, 0, 0, 1, 0, 0, 0, 0, 0, 1, 0)/\sqrt{2}$	$u_{383}$
	$\underline{T}_1$	$(0, 0, 0, 0, 1, 0, 1, 0, 0, 0, 0)/\sqrt{2}$	$u_{384}$
	$\underline{T}_4$	$(1, 0, 0, 0, 0, 0, 0, 0, 0, 1, 0)/\sqrt{2}$	$u_{385}$
	$\underline{T}_4$	$(0, 0, 1, 0, 0, 0, 0, 0, 1, 0, 0)/\sqrt{2}$	$u_{386}$
$S$	$\underline{T}_4$	$(0, 0, 0, 0, 1, 0, 1, 0, 0, 0, 0)/\sqrt{2}$	$u_{387}$
	$\underline{T}_4$	$(0, 1, 0, 0, 0, 0, 0, 0, 0, 0, -1)/\sqrt{2}$	$u_{388}$
	$\underline{T}_4$	$(0, 0, 0, 1, 0, 0, 0, 0, 0, -1, 0)/\sqrt{2}$	$u_{389}$
	$\underline{T}_4$	$(0, 0, 0, 0, 1, 0, -1, 0, 0, 0, 0)/\sqrt{2}$	$u_{390}$
	$\underline{S}_1$	$(1, 0, 0, 0, 0, 0, 0, 0, 0, 1, 0)/\sqrt{2}$	$u_{391}$
		$(-i, 0, 0, 0, 0, 0, 0, 0, 0, i, 0)/\sqrt{2}$	$u_{392}$
	$\underline{S}_1$	$(0, 0, 1, 0, 0, 0, 0, 0, 1, 0, 0)/\sqrt{2}$	$u_{393}$
		$(0, 0, -i, 0, 0, 0, 0, 0, i, 0, 0)/\sqrt{2}$	$u_{394}$
	$\underline{S}_1$	$(0, 0, 0, 0, 1, 0, 1, 0, 0, 0, 0)/\sqrt{2}$	$u_{395}$
		$(0, 0, 0, 0, -i, 0, i, 0, 0, 0, 0)/\sqrt{2}$	$u_{396}$
$S$	$\underline{S}_1$	$(0, 1, 0, 0, 0, 0, 0, 0, 0, -1)/\sqrt{2}$	$u_{397}$
		$(0, -i, 0, 0, 0, 0, 0, 0, 0, i)/\sqrt{2}$	$u_{398}$
	$\underline{S}_1$	$(0, 0, 0, 1, 0, 0, 0, 0, -1, 0)/\sqrt{2}$	$u_{399}$
		$(0, 0, 0, -i, 0, 0, 0, 0, i, 0)/\sqrt{2}$	$u_{400}$
	$\underline{S}_1$	$(0, 0, 0, 0, 0, 1, 0, -1, 0, 0, 0)/\sqrt{2}$	$u_{401}$
		$(0, 0, 0, 0, 0, -i, 0, i, 0, 0, 0)/\sqrt{2}$	$u_{402}$

TABLE VI. (Continued.)

$T'$	$T'_1$	$(1,0,0,0,0,0,-1,0,0,0,0,0)/\sqrt{2}$	$u_{403}$
	$T'_1$	$(0,0,1,0,0,0,0,0,0,-1,0)/\sqrt{2}$	$u_{404}$
	$T'_1$	$(0,0,0,0,1,0,0,0,-1,0,0,0)/\sqrt{2}$	$u_{405}$
	$T'_1$	$(0,1,0,0,0,0,0,1,0,0,0,0)/\sqrt{2}$	$u_{406}$
	$T'_1$	$(0,0,0,1,0,0,0,0,0,0,1,0)/\sqrt{2}$	$u_{407}$
	$T'_1$	$(0,0,0,0,0,1,0,0,0,1,0,0)/\sqrt{2}$	$u_{408}$
	$T'_4$	$(1,0,0,0,0,0,1,0,0,0,0,0)/\sqrt{2}$	$u_{409}$
	$T'_4$	$(0,0,1,0,0,0,0,0,0,1,0)/\sqrt{2}$	$u_{410}$
	$T'_4$	$(0,0,0,0,1,0,0,0,1,0,0,0)/\sqrt{2}$	$u_{411}$
	$T'_4$	$(0,1,0,0,0,0,0,-1,0,0,0,0)/\sqrt{2}$	$u_{412}$
	$T'_4$	$(0,0,0,1,0,0,0,0,0,0,0,-1)/\sqrt{2}$	$u_{413}$
	$T'_4$	$(0,0,0,0,0,1,0,0,0,-1,0,0)/\sqrt{2}$	$u_{414}$
$S'$	$S'_1$	$(1,0,0,0,0,0,1,0,0,0,0,0)/\sqrt{2}$	$u_{415}$
		$(-i,0,0,0,0,0,i,0,0,0,0,0)/\sqrt{2}$	$u_{416}$
	$S'_1$	$(0,0,1,0,0,0,0,0,0,1,0)/\sqrt{2}$	$u_{417}$
		$(0,0,-i,0,0,0,0,0,0,i,0)/\sqrt{2}$	$u_{418}$
	$S'_1$	$(0,0,0,0,1,0,0,0,1,0,0,0)/\sqrt{2}$	$u_{419}$
		$(0,0,0,0,-i,0,0,0,i,0,0,0)/\sqrt{2}$	$u_{420}$
	$S'_1$	$(0,1,0,0,0,0,0,-1,0,0,0,0)/\sqrt{2}$	$u_{421}$
		$(0,-i,0,0,0,0,0,-i,0,0,0,0)/\sqrt{2}$	$u_{422}$
	$S'_1$	$(0,0,0,1,0,0,0,0,0,0,-1)/\sqrt{2}$	$u_{423}$
		$(0,0,0,-i,0,0,0,0,0,0,-i)/\sqrt{2}$	$u_{424}$
$\Sigma$	$S'_1$	$(0,0,0,0,0,1,0,0,0,-1,0,0)/\sqrt{2}$	$u_{425}$
		$(0,0,0,0,0,-i,0,0,0,-i,0,0)/\sqrt{2}$	$u_{426}$
	$\Sigma_1$	$(1,0,0,0,0,0,0,0,0,0,0,0)$	$u_{427}$
	$\Sigma_1$	$(0,0,0,0,0,0,1,0,0,0,0,0)$	$u_{428}$
	$\Sigma_1$	$(0,0,1,0,1,0,0,0,0,0,0,0)/\sqrt{2}$	$u_{429}$
	$\Sigma_1$	$(0,0,0,0,0,0,0,0,1,0,1,0)/\sqrt{2}$	$u_{430}$
	$\Sigma_1$	$(0,0,0,1,0,-1,0,0,0,0,0,0)/\sqrt{2}$	$u_{431}$
	$\Sigma_1$	$(0,0,0,0,0,0,0,0,0,1,0,-1)/\sqrt{2}$	$u_{432}$
	$\Sigma_4$	$(0,1,0,0,0,0,0,0,0,0,0,0)$	$u_{433}$
	$\Sigma_4$	$(0,0,0,0,0,0,0,1,0,0,0,0)$	$u_{434}$
	$\Sigma_4$	$(0,0,0,1,0,1,0,0,0,0,0,0)/\sqrt{2}$	$u_{435}$
	$\Sigma_4$	$(0,0,0,0,0,0,0,0,0,1,0,1)/\sqrt{2}$	$u_{436}$
$R$	$\Sigma_4$	$(0,0,1,0,-1,0,0,0,0,0,0,0)/\sqrt{2}$	$u_{437}$
	$\Sigma_4$	$(0,0,0,0,0,0,0,0,0,1,0,-1)/\sqrt{2}$	$u_{438}$
	${}^1E'$	$(1,0,0,0,0,0,0,0,0,0,0,0)$	$u_{439}$
	${}^1E'$	$(0,0,1,0,1,0,0,0,0,0,0,0)/\sqrt{2}$	$u_{440}$
	${}^1E'$	$(0,0,0,1,0,-1,0,0,0,0,0,0)/\sqrt{2}$	$u_{441}$
	${}^2E'$	$(0,0,0,0,0,0,1,0,0,0,0,0)$	$u_{442}$
	${}^2E'$	$(0,0,0,0,0,0,0,0,1,0,1,0)/\sqrt{2}$	$u_{443}$
	${}^2E'$	$(0,0,0,0,0,0,0,0,0,1,0,-1)/\sqrt{2}$	$u_{444}$
	${}^1E''$	$(0,0,0,0,0,0,0,1,0,0,0,0)$	$u_{445}$
	${}^1E''$	$(0,0,0,0,0,0,0,0,0,1,0,1)/\sqrt{2}$	$u_{446}$
	${}^1E''$	$(0,0,0,0,0,0,0,0,1,0,-1,0)/\sqrt{2}$	$u_{447}$
	${}^2E''$	$(0,1,0,0,0,0,0,0,0,0,0,0)$	$u_{448}$
	${}^2E''$	$(0,0,0,1,0,1,0,0,0,0,0,0)/\sqrt{2}$	$u_{449}$
	${}^2E''$	$(0,0,1,0,-1,0,0,0,0,0,0,0)/\sqrt{2}$	$u_{450}$

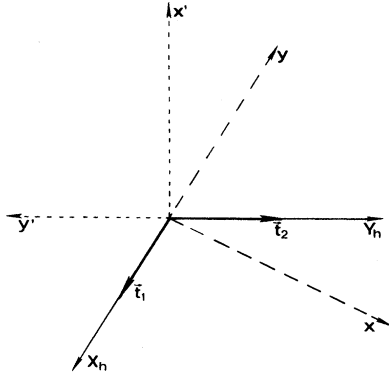


FIG. 2. Relative orientation of the axes  $x, y, z$  and  $x', y', z'$  used in the text with respect to the hexagonal axes.

cells the displacements are given by

$$u_{\alpha}(lR) = E_{\alpha}(R | \vec{K}_1 n t a) \exp[i \vec{K}_1 \cdot \vec{x}(l)] . \quad (12)$$

The tabulated symmetry modes correspond to the small IR of the different stars. To obtain the symmetry-adapted modes for the corresponding IR of  $P6_3/mmc$ , it is only required to make use of Eq. (9). The generators of the star arms are listed in Appendix A and coincide with those chosen for the symmetry points in Ref. 6. The matrices  $\Gamma$  for these generators to be used in (9) are shown in Appendix C.

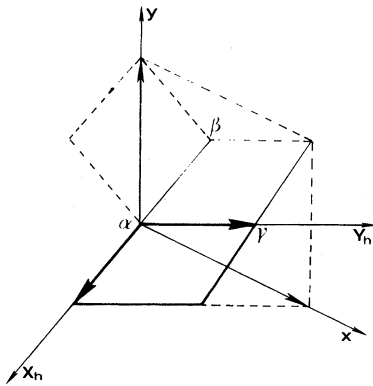


FIG. 3. Relationship between the Bravais lattice ( $T_d$ ) for the  $\text{KNiCl}_3$  at room temperature and the prototype lattice ( $T$ ) corresponding to the hexagonal perovskite structure.  $\alpha$ ,  $\beta$ , and  $\gamma$  are the origin of the three cells included in the high-temperature cell. The relations between coordinates are  $X_h = x - 2y$  and  $Y_h = 2x - y$ , where  $x$  and  $y$  are the reference frame for the low-symmetry phase.

TABLE VII. Symmetry modes of the hexagonal perovskite structure ( $2L$ ) compatible with the symmetry  $P6_3cm$  ( $T_d$ ) of the  $\text{KNiCl}_3$  room-temperature structure.

		$A_z$	$A_{xy}$	$B_z$	$B_{xy}$	$X_z$	$X_{xy}$
$K$	$K_4$	1				1	
	$K_1$				1		2
$\Gamma$	$A_{1g}$						1
	$A_{2u}$	1		1		1	

#### IV. DISTORTION ANALYSIS OF THE $\text{KNiCl}_3$ STRUCTURE AT ROOM TEMPERATURE

The crystal structure of  $\text{KNiCl}_3$  at room temperature has been recently determined by x-ray single-crystal diffraction techniques.<sup>5</sup> It can be considered as a slight modification with symmetry  $P6_3cm$  of the hexagonal perovskite ( $2L$ ) structure, which is the usual arrangement of this type of compounds at high temperatures. A first-order structural phase transition is known to occur in  $\text{KNiCl}_3$  at 753 K, and there is probably another one at 560 K.<sup>5</sup> Both high-temperature phases are hexagonal, but their structures have not been reported yet. It is most likely that hexagonal perovskite is one of them. In any case, as with other compounds of the same family, it is reasonable to consider hexagonal perovskite ( $\text{CsNiCl}_3$ ) as the prototype phase structure for the  $\text{KNiCl}_3$  room-temperature arrangement.

In order to see a practical use of the results from

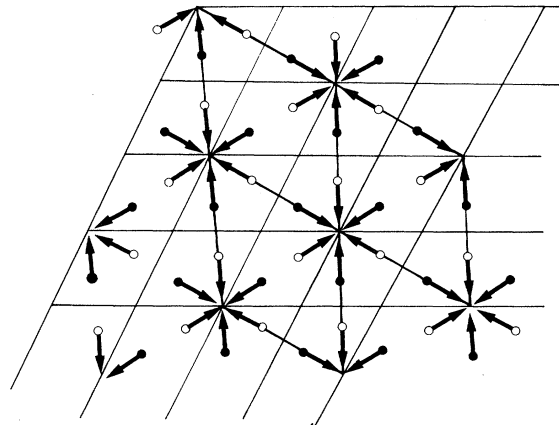


FIG. 4. Schematic representation of mode  $\phi_5$  with symmetry  $K_1(1,1)$  for the  $B$  ions ( $K$  in  $\text{KNiCl}_3$ ).

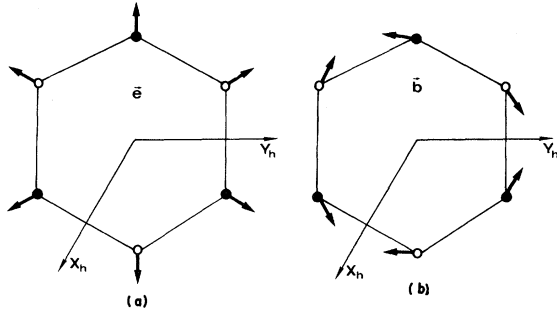


FIG. 5. Schematic representation of displacements (a)  $\vec{e}$  and (b)  $\vec{b}$  for the  $X$  ions mentioned in the text.

the previous sections and the tables in Ref. 6, in this section we shall study the distortion that relates these two phases. The different symmetry modes present in the distortion are determined and described. Afterwards we discuss their relative weight in the actual distortion, making use of the published room-temperature structural data.

The relationship between the prototype ( $T$ ) and distorted phase ( $T_d$ ) hexagonal lattices, in this particular case, is shown in Fig. 3. A tripling of the unit cell takes place and their orientation differs by an angle of  $90^\circ$ . According to Tables 2 and 3 in Ref. 6, the  $T_a$  lattice is associated with the symmetry point  $K$  of the hexagonal Brillouin zone and IR  $K_4$  should be the symmetry of the OP [being its displacement along the  $(1, -1)$  direction], if  $P6_3cm$  is to be the symmetry of the low-symmetry phase.

According to what has been stated in Sec. II there are other IR's compatible with the low-symmetry phase. They are those which have, as invariance groups, subgroups of  $P6_3/mmc$  containing the group  $P6_3cm$  ( $T_a$ ). They can be readily

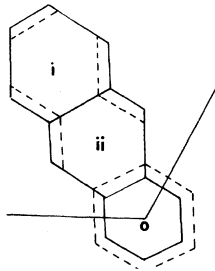


FIG. 6. Distortion in the free volumen surrounding the  $X$  ions created by mode  $\phi_5$  [symmetry  $K_1(1,1)$ ] of the  $B$  ions.

TABLE VIII. Displacement vectors in the three relevant unit cells ( $1=0,1,2$ ) for modes  $\phi_6$  and  $\phi_7$  of symmetry  $K_1(1,1)$ .

$X_{xy}$	$u(0)$	$u(1)$	$u(2)$
$\phi_6$	$2\vec{e}$	$-\vec{e}$	$-\vec{e}$
$\phi_7$	0	$\vec{b}$	$-\vec{b}$

sorted out in Table 3 of Ref. 6. Apart from the trivial representation, they are  $A_{2u}$  with invariance group  $P6_3mc$  ( $T$ ) and  $K_1$  [direction  $(1,1)$ ] with invariance group  $P6_3/mcm$  ( $T_a$ ) (Ref. 6). This means that only modes with symmetry  $K_4(1, -1)$ ,  $K_1(1,1)$ ,  $A_{2u}$ , and  $A_{1g}$  will be present in the crystal distortion. The number of modes with these symmetries and their corresponding subspaces, as obtained from Appendix B, are shown in Table VII. From this table we can see that nine degrees of freedom are involved in the problem. We shall now describe the atomic displacements corresponding to each of them. We first present the explicit calculation for the mode  $K_1$  in the  $B_{xy}$  subspace, as an example of the use of the tables introduced in the preceding section.

The basis vectors for the IR  $K_1$  are as follows (Table IV):

$$\vec{E}(\vec{k}_1, \vec{K}_1, 1, 1) = U_{137}, \quad (13)$$

$$\vec{E}(\vec{k}_2, K_1, 1, 1) = \Gamma(\vec{k}_1; \{I \mid 000\}) \vec{E}(\vec{k}_1, K_1, 1, 1),$$

where  $\vec{k}_1 = (-\frac{1}{3}, \frac{2}{3}, 0)$  and  $\vec{k}_2 = (\frac{1}{3}, -\frac{2}{3}, 0)$  are the two arms of the  $k$  star (Table XIII, Appendix A). The matrix  $\Gamma$  in (13), according to Appendix C, is

TABLE IX. Description of the symmetry modes  $\phi_8$  and  $\phi_9$  of symmetry  $K_4(1, -1)$  for the three relevant unit cells.

		$u(0)$	$u(1)$	$u(2)$
$\phi_8$	$A_{1z}$	2	-1	-1
	$A_{2z}$	2	-1	-1
$\phi_9$	$X_{1z}$	2	-1	-1
	$X_{2z}$	2	-1	-1
	$X_{3z}$	2	-1	-1
	$X_{4z}$	2	-1	-1
	$X_{5z}$	2	-1	-1
	$X_{6z}$	2	-1	-1

TABLE X. Distortion of the room-temperature structure with respect to the ideal hexagonal perovskite structure (2L). The axes used are the orthogonal ones introduced in Sec. III. The numbers in parentheses besides *A*, *B*, and *X* labels indicate the unit-cell label from the prototype Bravais lattice in which the ion is situated. The numbers in parentheses besides *K*, *Ni*, and *Cl* labels follow the notation used in Ref. 5.

	<i>X</i>	<i>Y</i>	<i>Z</i>	
<i>B</i> <sub>1</sub> (2)	$\sqrt{3}$	3	79.4	<i>K</i>
<i>A</i> <sub>1</sub> (0)				<i>Ni</i> (1)
<i>A</i> <sub>1</sub> (2)			123	<i>Ni</i> (2)
<i>X</i> <sub>1</sub> (0)	$(\sqrt{3}/2)(319.6-2x)$		10.4	<i>Cl</i> (1)
<i>X</i> <sub>3</sub> (1)	$(\sqrt{3}/2)(x-162)$	$-240.2+\frac{3}{2}x$	135.2	<i>Cl</i> (2)

given by

$$\Gamma(\vec{k}_1; \{I | 000\}) = \Lambda_3(\vec{k}_1) \begin{bmatrix} I \\ I \end{bmatrix}, \quad (14)$$

where  $\Lambda_3(\vec{k}_1) = \exp(-2\pi i/3) = \omega^*$ . Using (13) and (14) we obtain

$$\vec{E}(\vec{k}_2, K_1, 1, 1) = \frac{1}{2}(\omega, i\omega, -\omega^*, i\omega^*). \quad (15)$$

The displacements corresponding to the (1,1) subspace in *K* are then (for *l*=0 unit cell):

$$\begin{aligned} \vec{U}(0) &= \vec{E}(\vec{k}_1, K_1, 1, 1) + \vec{E}(\vec{k}_2, K_1, 1, 1) \\ &= \frac{1}{2}\omega^*(-1, \sqrt{3}, -2, 0). \end{aligned} \quad (16)$$

As the transition triplicates the unit cell, displacements of three adjacent unit cells in the prototype phase must be considered in order to describe the distortion. Using Eq. (12) with  $\vec{x}(1) = (1, 0, 0)$  and  $\vec{x}(2) = (1, 1, 0)$ , we find in an analogous way to

$$\phi_4 = u_{271} = \frac{1}{2\sqrt{6}}(2, 0, -1, \sqrt{3}, -1, -\sqrt{3}, -2, 0, 1 - \sqrt{3}, 1, \sqrt{3}). \quad (19)$$

TABLE XI. Amplitudes of the nine modes intervening in the room-temperature distortion of  $\text{KNiCl}_3$ .

Mode	Symmetry	Subspace	Amplitude	Faintness index
$\phi_1$	$A_z$	$A_{2u}$	-5.5	3
$\phi_2$	$B_z$	$A_{2u}$	-8	3
$\phi_3$	$X_z$	$A_{2u}$	+6	3
$\phi_4$	$X_{xy}$	$A_{1g}$	unknown	2
$\phi_5$	$B_{xy}$	$K_1(1, 1)$	-1.7	2
$\phi_6$	$X_{xy}$	$K_1(1, 1)$	-0.5	2
$\phi_7$	$X_{xy}$	$K_1(1, 1)$	-1.4	2
$\phi_8$	$A_z$	$K_4(1, -1)$	-41	1
$\phi_9$	$X_z$	$K_4(1, -1)$	-41.6	1

$\vec{u}(0)$ :

$$\begin{aligned} \vec{u}(1) &= \frac{1}{2}\omega^*(2, 0, 1, -\sqrt{3}), \\ \vec{u}(2) &= \frac{1}{2}\omega^*(-1, \sqrt{3}, 1, \sqrt{3}). \end{aligned} \quad (17)$$

In Fig. 4 the  $K_1$  distortion  $\phi_5 = \vec{u}(0) + \vec{u}(1) + \vec{u}(2)$  in the  $b_{xy}$  subspace is schematically shown. In this figure, more than three cells are included in order to see the distortion effect. We observe that the *B* ions try to “tighten up” around the lattice site axes that are kept in the low-symmetry phase. When the amplitude mode is negative, the effect will be reverse. It can be considered a breathing mode of the octahedra columns of *B* ions around the lattice site axes which are conserved. Note that in fact no lattice site is “privileged” if the antiphase domain structure is considered.<sup>6,16</sup> The remaining eight modes are obtained in a similar way. A short description of them is given below.

#### 1. $A_{2u}$ modes

The three  $A_{2u}$  modes correspond to movements of all the atoms along the *z* axis. In this case the IR belongs to the  $\Gamma$  point; all unit cells in the *T* lattice are in phase and the IR is one-dimensional. Therefore, the corresponding atomic displacements can be easily read in the tables:

$$\phi_1 = u_1, \quad \phi_2 = u_{31}, \quad \phi_3 = u_{181}, \quad (18)$$

It is important to note that in this distortion, the relative displacements between different groups of atoms could induce a spontaneous polarization.

#### 2. $A_{1g}$ modes

There exists a unique  $A_{1g}$  mode that corresponds to displacements of the *X* atoms on the *xy* plane:

TABLE XII. Reciprocal-lattice vectors of the hexagonal Bravais lattice and their transformation properties by application of the chosen generators.

$E$	$\vec{g}_1 = \frac{2\pi}{a}(1/\sqrt{3}, -1, 0)$	$\vec{g}_2 = \frac{2\pi}{a}(2/\sqrt{3}, 0, 0)$	$\vec{g}_3 = \frac{2\pi}{a}(0, 0, 1)$
$C_6^+$	$\vec{g}_2$	$-\vec{g}_1 + \vec{g}_2$	$\vec{g}_3$
$C_2$	$-\vec{g}_1$	$-\vec{g}_2$	$\vec{g}_3$
$I$	$-\vec{g}_1$	$-\vec{g}_2$	$-\vec{g}_3$

It corresponds to a “breathing” of the  $X$  octahedra columns around the  $z$  axis, while keeping the  $P6_3/mmc$  symmetry. It is schematically shown in Fig. 5(a). This type of distortion for a unit cell will be in what follows indicated by the symbol  $\vec{e}$ .

### 3. $K_1$ modes

Apart from the  $K_1$  mode, which was determined above, there are two others associated to  $X_{xy}$  displacements. They are shown in Table VIII. Vectors  $\vec{e}$  and  $\vec{b}$  of this table are shown in Fig. 5. It is interesting to analyze the distortion under the action of the three modes together. In Fig. 6 we

show a schematic representation, for the three relevant lattice sites, of the distortion created by mode  $\phi_5$  in the surrounding of the  $X$  ions. The  $\vec{e}$  displacements in  $\phi_6$  (Table VIII) can be considered as expansions and contractions of the  $X$  octahedra columns, in order to adequate themselves to the volume change of the surrounding free space. The same occurs with the  $\vec{b}$  displacement in  $\phi_7$ , which can be interpreted as a result of the geometric change of these surroundings. Note that for  $l=0$ , no displacement is present in  $\phi_7$ , in agreement with the fact that the point symmetry of the surrounding  $B$  ions is maintained by mode  $\phi_5$  for this unit cell, as can be seen in Fig. 6. From this “mechanical” point of view, it is expected that the  $\phi_6$  ampli-

TABLE XIII. Symmetry points and lines of the hexagonal Brillouin lattice studied in this paper. The number of arms in the star and chosen generators are also indicated. The vector components are shown in the basis  $g_1, g_2, g_3$ .

Point or line	$k_1$ components	Arms	Generators
$\Gamma$	(0,0,0)	1	
$M$	$(0, \frac{1}{2}, 0)$	3	$C_6^+$
$A$	$(0, 0, \frac{1}{2})$	1	
$L$	$(0, \frac{1}{2}, \frac{1}{2})$	3	$C_6^+$
$K$	$(\frac{1}{3}, \frac{2}{3}, 0)$	2	$I$
$H$	$(\frac{1}{3}, \frac{2}{3}, \frac{1}{2})$	2	$I$
$\Delta(A)$	$(0, 0, \alpha)$	2	$I$
$U(ML)$	$(0, \frac{1}{2}, \alpha)$	6	$C_6^+, I$
$P(KH)$	$(\frac{1}{3}, \frac{2}{3}, \alpha)$	4	$C_2, I$
$T(\Gamma K)$	$(\bar{\alpha}, 2\alpha, 0)$	6	$C_6^+$
$S(AH)$	$(\bar{\alpha}, 2\alpha, \frac{1}{2})$	6	$C_6^+$
$T'(MK)$	$(2\bar{\alpha}, \frac{1}{2} + \alpha, 0)$	6	$C_6^+$
$S'(LH)$	$(2\alpha, \frac{1}{2} + \alpha, \frac{1}{2})$	6	$C_6^+$
$\Sigma(\Gamma M)$	$(0, \alpha, 0)$	6	$C_6^+$
$R(AL)$	$(0, \alpha, \frac{1}{2})$	6	$C_6^+$

TABLE XIV. Compatibility relations for the symmetry modes corresponding to the  $A$  ions in the hexagonal perovskite structure ( $2L$ ).

$\Gamma$	$\Delta$	$A$	$R$	$L$	$U$	$M$	$\Sigma$	$\Gamma$	$A \times i_3$
$A_{1u}$	$A_1$	$A_1$	$E'$	$L_1$	$U_1$	$M_1$	$\Sigma_1$	$A_{1u}$	$z$
$B_{1u}$	$B_1$	$A_1$	$E'$	$L_1$	$U_1$	$M_1$	$\Sigma_1$	$B_{1u}$	
$E_{2u}$	$E_2$	$A_2$	$E'$	$L_2$	$U_2$	$M_2$	$\Sigma_2$	$E_{2u}$	$x$
$E_{4u}$	$E_4$	$A_2$	$E''$	$L_2$	$U_2$	$M_2$	$\Sigma_2$	$E_{4u}$	$y$
$\Gamma$	$T$	$K$	$P$	$H$	$S$	$A$			
$A_{2u}$	$T_2$	$K_4$	$P_4$	$H_3$	$S_4$	$A_4$			$z$
$B_{2u}$	$T_4$	$K_2$	$P_2$	$H_3$	$S_4$	$A_4$			$x'$
$E_{2u}$	$T_2$	$K_6$	$P_3$	$H_2$	$S_3$	$A_3$			$y'$
$E_{4u}$	$T_4$	$K_2$	$P_3$	$H_2$	$S_3$	$A_3$			
$L$	$S'$	$H$							
$L_1$	$S'_1$	$H_3$							$z$
$L_2$	$S'_2$	$H_1$							$x$
$L_3$	$S'_3$	$H_2$							$y$
$M$	$T'$	$K$							
$M_1$	$T'_1$	$K_4$							$z$
$M_2$	$T'_2$	$K_2$							$x$
$M_3$	$T'_3$	$K_6$							$y$
$M_4$	$T'_4$	$K_2$							
$M_5$	$T'_5$	$K_3$							
$M_6$	$T'_6$	$K_1$							

TABLE XV. Compatibility relations for the symmetry modes corresponding to the  $B$  ions in the hexagonal perovskite structure ( $2L$ ).

$\Gamma$	$\Delta$	$A$	$R$	$L$	$U$	$M$	$\Sigma$	$\Gamma$	$A \times i_3$
$B_{2g}$	$B_2$	$A_2$	$E'$	$L_2$	$U_2$	$M_2$	$\Sigma_2$	$B_{2g}$	$z$
$A_{2g}$	$A_2$	$A_2$	$E'$	$L_2$	$U_2$	$M_2$	$\Sigma_2$	$A_{2g}$	$x$
$E_{2g}$	$E_2$	$A_2$	$E'$	$L_2$	$U_2$	$M_2$	$\Sigma_2$	$E_{2g}$	$y$
$E_{4g}$	$E_4$	$A_2$	$E''$	$L_2$	$U_2$	$M_2$	$\Sigma_2$	$E_{4g}$	
$\Gamma$	$T$	$K$	$P$	$H$	$S$	$A$			
$B_{2g}$	$T_2$	$K_6$	$P_3$	$H_2$	$S_3$	$A_3$			$z$
$A_{2g}$	$T_2$	$K_6$	$P_3$	$H_2$	$S_3$	$A_3$			$x'$
$E_{2g}$	$T_2$	$K_2$	$P_3$	$H_2$	$S_3$	$A_3$			$y'$
$E_{4g}$	$T_4$	$K_2$	$P_3$	$H_2$	$S_3$	$A_3$			
$L$	$S'$	$H$							
$L_1$	$S'_1$	$H_3$							$z$
$L_2$	$S'_2$	$H_1$							$x$
$L_3$	$S'_3$	$H_2$							$y$
$M$	$T'$	$K$							
$M_1$	$T'_1$	$K_6$							$z$
$M_2$	$T'_2$	$K_2$							$x$
$M_3$	$T'_3$	$K_6$							$y$
$M_4$	$T'_4$	$K_2$							
$M_5$	$T'_5$	$K_3$							
$M_6$	$T'_6$	$K_1$							

TABLE XVI. Compatibility relations for the symmetry modes along the  $z$  axis corresponding to the  $X$  ions in the hexagonal perovskite structure ( $2L$ ).

$\Gamma$	$\Delta$	$A$	$R$	$L$	$U$	$M$	$\Sigma$	$\Gamma$
$A_{1u}$	$A_1$	$A_1$	$E'$	$L_1$	$U_1$	$M_1$	$\Sigma_1$	$A_{1u}$
$B_{1u}$	$B_1$	$A_1$	$E'$	$L_1$	$U_1$	$M_1$	$\Sigma_1$	$B_{1u}$
$E_{2u}$	$E_2$	$A_2$	$E'$	$L_2$	$U_2$	$M_2$	$\Sigma_2$	$E_{2u}$
$E_{4u}$	$E_4$	$A_2$	$E''$	$L_2$	$U_2$	$M_2$	$\Sigma_2$	$E_{4u}$
$\Gamma$	$T$	$K$	$P$	$H$	$S$	$A$		
$A_{2u}$	$T_2$	$K_4$	$P_4$	$H_3$	$S_4$	$A_4$		
$B_{2u}$	$T_4$	$K_2$	$P_2$	$H_3$	$S_4$	$A_4$		
$E_{2u}$	$T_2$	$K_6$	$P_3$	$H_2$	$S_3$	$A_3$		
$E_{4u}$	$T_4$	$K_2$	$P_3$	$H_2$	$S_3$	$A_3$		
$L$	$S'$	$H$						
$L_1$	$S'_1$	$H_3$						
$L_2$	$S'_2$	$H_1$						
$L_3$	$S'_3$	$H_2$						
$M$	$T'$	$K$						
$M_1$	$T'_1$	$K_4$						
$M_2$	$T'_2$	$K_2$						
$M_3$	$T'_3$	$K_6$						
$M_4$	$T'_4$	$K_2$						
$M_5$	$T'_5$	$K_3$						
$M_6$	$T'_6$	$K_1$						

tude has a sign opposite to that of  $\phi_5$ , while  $\phi_7$  has the same sign.

#### 4. $K_4$ modes

The two  $K_4$  modes are indicated in Table IX. In this case the atoms  $A$ , in the center of the  $B$  octahedra columns, show displacements with amplitude twice as large as that for atoms between columns. Moreover, both displacements have opposite directions.

Since  $K_4 (1, -1)$  is the symmetry of the OP, if the phase transition is of the displacive type, the soft mode will be given by a linear combination of these two  $K_4$  modes. Furthermore, its amplitude will be proportional to  $(T - T_0)^{1/2}$  when a second character is shown.

In summary, the structural distortion of the hexagonal perovskite structure corresponding to a  $P6_3cm(T_a)$  symmetry can be schematically represented as

$$u = \sum_{i=1}^g c_i \phi_i,$$

TABLE XVII. Compatibility relations for the symmetry modes in the  $xy$  plane corresponding to the  $X$  ions in the hexagonal perovskite structure ( $2L$ ).

$\Gamma$	$\Delta$	$\Pi$	$R$	$L$	$U$	$M$	$\Sigma$	$\Gamma$	$A_{X15}$
$A_{1g}$ $B_{1u}$	$A_1$ $B_1$	$A_1$ $B_1$	$2E'$ $2E''$	$2L_1$ $L_2$	$2U_1$ $U_3$	$2M_1^+$ $M_3^+$	$4\Sigma_1$ $2\Sigma_4$	$A_{1g}$ $B_{1u}$	$\times$
$2E_{1u}$ $2E_{2g}$	$2E_1$ $2E_2$	$2H_3$ $3E'' + 3E''$	$2E'$ $2E''$	$L_1$ $L_2$	$U_1$ $U_2$	$M_1^+$ $M_2^+$	$2\Sigma_1$ $2\Sigma_4$	$2E_{1u}$ $2E_{2g}$	$y$
$A_{2g}$ $B_{2u}$	$A_2$ $B_2$	$A_2$ $B_2$	$2E'$ $2E''$	$L_1$ $L_2$	$U_1$ $U_2$	$M_1^+$ $M_2^+$	$2\Sigma_1$ $2\Sigma_4$	$A_{2g}$ $B_{2u}$	$y$
$\Gamma$	$T$	$K$	$P$	$H$	$S$	$A$			
$A_{1g}$ $B_{1u}$	$3T_1$ $3T_4$	$6T_1$ $6T_4$	$2K_1$ $4K_5$	$2P_1$ $4P_3$	$3S_1$ $6S_1$	$A_1$ $2H_3$	$\times'$		
$2E_{1u}$ $2E_{2g}$	$3T_1$ $3T_4$	$6T_1$ $6T_4$	$2K_1$ $4K_5$	$2P_1$ $4P_3$	$3S_1$ $6S_1$	$A_1$ $2H_3$	$y'$		
$A_{2g}$ $B_{2u}$	$3T_1$ $3T_4$	$6T_1$ $6T_4$	$2K_1$ $4K_5$	$2P_1$ $4P_3$	$3S_1$ $6S_1$	$A_1$ $2H_3$			
$L$	$S'$	$H$	$M$	$T'$	$K$				
$2L_1$ $L_2$	$3S_1$ $16S_1$	$2H_1$ $2H_3$	$2M_1^+$ $M_2^-$	$3T_1$ $3T_4$	$2K_1$ $4K_5$	$\times$			
$L_1$ $2L_2$	$3S_1$ $3S_1'$	$2H_1$ $2H_2$	$M_3^+$ $M_4^+$	$3T_1$ $3T_4$	$2K_1$ $2K_2$	$y$			

where  $\phi_i$  are the modes discussed above. In our particular case the distortion  $u$  can be obtained from the experimental structural data.<sup>5</sup> for this purpose, it is only necessary to operate with the asymmetrical unit in the room-temperature structure of  $\text{K}(\text{NO}_3)_3$ . The results are shown in Table X. The atom displacements with respect to their ideal position in the hexagonal perovskite structure are indicated as fractions of the corresponding cell parameters, along the orthogonal axes used in previous sections (see Fig. 2). The displacements of the Cl ions are indeterminable owing to the fact that their position is not fixed by symmetry conditions in the prototype phase (see Fig. 1).

The subsequent determination of the amplitudes

$c_i$  intervening in (20) is straightforward owing to the orthogonality between the different modes  $\phi_i$ . We summarize the results in Table XI, where the faintness index for every mode is also indicated. In order to be able to make a meaningful comparison of the amplitudes, the usual normalization factors shown in Tables II–IV for the different modes have not been considered. Hence the metric chosen in this way is therefore, in some sense, arbitrary, but it allows a qualitative indication of the relative weight of their contributions to the total atomic displacements, since the atomic displacements intervening in any mode are of the same order of magnitude. Obviously, no mass-dependent normalization has been used. It is important to

note that the amplitude of the  $A_{1g}$  modes in Table XI remains unknown. This indetermination for  $A_{1g}$  modes will be usual in any analysis of this type when the actual parent phase structure is unknown with respect to those atomic positions that are not fixed by symmetry conditions. It should be also pointed out that in the case of  $A_{2u}$  modes, the amplitudes have been calculated considering the center of mass of every proton-type unit cell at rest for this type of mode.

Some important points can be deduced from Table XI. First, the predominance of modes  $K_4$  in the distortion is evident, being at least 1 order of magnitude stronger. Although these modes correspond to the OP symmetry for the assumed phase transition, their strong contribution to the total distortion at a temperature separated by about 260 K from the nearest suggested phase transition<sup>5</sup> is rather significant, and suggests that the OP contributions to the structural distortion created in a phase transition remain much stronger than those produced as a coupling effect even for temperatures rather distant from the transition point. This suggestion is more significant if we consider that, from a group-theoretical point of view, all the modes listed compatible with the new symmetry have the same importance in describing the final distortion.

On the other hand, the contribution of modes with faintness index 2 seems to have less importance than those having faintness index 3, in contradiction to what it should be if we consider that the faintness index is a measure of the coupling strength with the OP.

Finally, with respect to the sign correlation between modes  $\phi_5$ ,  $\phi_6$ , and  $\phi_7$ , which was suggested above from geometric considerations, the sign of  $\phi_6$  is in agreement with it, but not the one for  $\phi_7$ . In any case the amplitude of the three modes are not sufficiently significant to allow a clear test.

## APPENDIX A

In this appendix the characteristics of the hexagonal reciprocal lattice and its Brillouin zone are summarized in Tables XII and XIII following Ref. 8, and we indicate the generators we have chosen for every  $\vec{k}$  star.

## APPENDIX B

In this appendix the compatibility relations for the modes corresponding to the different ions are shown in Tables XIV–XVII.

## APPENDIX C

In this appendix we indicate the matrices  $\Gamma$  defined in (4) (Sec. II) for the generators chosen in Table XII.

$$\begin{array}{l}
 I \quad T_a C_2 \quad t_a C_6^+ \\
 A_{\text{atom}} \quad \begin{bmatrix} I & \\ & \Lambda_1 I \end{bmatrix} \quad \begin{bmatrix} & \Lambda_2 C_2 \\ C_2 & \end{bmatrix} \quad \begin{bmatrix} & \Lambda_1 C_6^+ \\ C_6^+ & \end{bmatrix} \\
 B_{\text{atom}} \quad \begin{bmatrix} & I \\ I & \end{bmatrix} \quad \begin{bmatrix} & \Lambda_5 C_2 \\ \Lambda_4 C_2 & \end{bmatrix} \quad \begin{bmatrix} & \Lambda_6 C_6^+ \\ C_6^+ & \end{bmatrix} \\
 X_{\text{atom}} \Lambda_1 \quad \begin{bmatrix} & & I & & \\ & & & I & \\ & & & & I \\ I & & & & \\ & I & & & \\ & & I & & \end{bmatrix} \quad \begin{bmatrix} & & \Lambda_2 C_2 & & \\ & & & \Lambda_2 C_2 & \\ & & & & \Lambda_2 C_2 \\ C_2 & & & & \\ & C_2 & & & \\ & & C_2 & & \end{bmatrix} \quad \begin{bmatrix} & & & & \Lambda_2 C_6^+ & \\ & & & & & \Lambda_2 C_6^+ \\ & & & & & \Lambda_2 C_6^+ \\ C_6^+ & & & & & \\ & C_6^+ & & & & \\ & & C_6^+ & & & \\ C_6^+ & & & & & \end{bmatrix}
 \end{array}$$

The vectorial representations for  $I$ ,  $C_2$ , and  $C_6^+$  are

$$I = \begin{bmatrix} -1 & & \\ & -1 & \\ & & -1 \end{bmatrix}, \quad C_2 = \begin{bmatrix} -1 & & \\ & -1 & \\ & & 1 \end{bmatrix}, \quad C_6^+ = \begin{bmatrix} \frac{1}{2} & -\frac{\sqrt{3}}{2} & 0 \\ \frac{\sqrt{3}}{2} & \frac{1}{2} & 0 \\ 0 & 0 & 1 \end{bmatrix},$$

and  $\Lambda_j = \exp(i\vec{k}\Gamma_j)$ , with  $T_1 = (0, 0, -1)$ ,  $T_2 = (0, 0, 1)$ ,  $T_3 = (-1, -1, -1)$ ,  $T_4 = (-1, -1, 0)$ ,  $T_5 = (-1, -1, 1)$ ,  $T_6 = (-1, 0, 1)$ .

<sup>1</sup>H. Arend, P. Muralt, S. Pleska, and D. Altermatt, *Ferroelectrics* **24**, 297 (1980); J. Fernandez, M. J. Tello, and M. A. Arriandiaga, *Mater. Res. Bull.* **13**, 477 (1978).

<sup>2</sup>C. J. Kroese and W. J. A. Maaskant, *Chem. Phys.* **5**, 224 (1974).

<sup>3</sup>A. Sawada, Y. Makita, and Y. Takagi, *J. Phys. Soc. Jpn.* **41**, 174 (1976).

<sup>4</sup>J. M. Pérez-Mato, J. L. Mañes, and M. J. Tello, *J. Phys. C* **13**, 2667 (1980).

<sup>5</sup>D. Visser, G. C. Verschorr, and D. J. Ijdo, *Acta Crystallogr. B* **36**, 28 (1980).

<sup>6</sup>J. M. Pérez-Mato, J. L. Mañes, M. J. Tello, and F. J. Zúñiga, *J. Phys. C* **14**, 1121 (1981).

<sup>7</sup>J. C. Tolédano and P. Tolédano, *Phys. Rev. B* **21**, 1139 (1980).

<sup>8</sup>C. J. Bradley and A. P. Cracknell, *The Mathematical Theory of Symmetry in Solids* (Clarendon, Oxford, 1972).

<sup>9</sup>A. A. Maradudin and S. H. Vosko, *Rev. Mod. Phys.* **40**, 1 (1968).

<sup>10</sup>L. D. Landau and E. M. Lifshitz, *Statistical Physics* (Pergamon, New York, 1969).

<sup>11</sup>Strains in the crystal Bravais lattice are neglected.

<sup>12</sup>V. Kopsky, *Ferroelectrics* **24**, 3 (1980).

<sup>13</sup>K. Aizu, *J. Phys. Soc. Jpn.* **35**, 1704 (1973).

<sup>14</sup>K. Aizu, *J. Phys. Soc. Jpn.* **36**, 1273 (1974).

<sup>15</sup>K. Aizu, *J. Phys. Soc. Jpn.* **37**, 885 (1974).

<sup>16</sup>C. Konak, V. Kopsky, and F. Smutny, *J. Phys. C* **11**, 2493 (1978).

<sup>17</sup>The symmetry points and lines of the hexagonal Brillouin zone studied in this paper, together with their  $k$ -vector components, number of arms in the star, and chosen generators are shown in Appendix A. In this appendix we also show the reciprocal-lattice vectors and their transformation properties by the application of the generators.